NOLTR 72-38

WAKE TRANSITION DATA BEHIND 22-DEGREE HALF-ANGLE CONES AT $M_\infty = 9.0$

By
Charles J. Infosino
Robert A. Leverance

21 JANUARY 1972

NOL

NAVAL ORDNANCE LABORATORY, WHITE OAK, SILVER SPRING, MARYLAND

NOLTR 72-38

UNCLASSIFIED

Security Classification

DOCUMENT CONTROL DATA - R & D

(Security classification of title, body of abstract and indexing annotation must be entered when the overall report is classified)

1. ORIGINATING ACTIVITY (Corporate author) Naval Ordnance Laboratory Silver Spring, Maryland 20910	2a. REPORT SECURITY CLASSIFICATION UNCLASSIFIED 2b. GROUP

3. REPORT TITLE

WAKE TRANSITION DATA BEHIND 22-DEGREE HALF-ANGLE CONES AT $M_\infty = 9.0$

4. DESCRIPTIVE NOTES (Type of report and inclusive dates)

5. AUTHOR(S) (First name, middle initial, last name)

Charles J. Infosino
Robert A. Leverance

6. REPORT DATE 21 January 1972	7a. TOTAL NO. OF PAGES 44	7b. NO. OF REFS 13
8a. CONTRACT OR GRANT NO. b. PROJECT NO. MAT-03L-000/ZR011-01-01 c. d.	9a. ORIGINATOR'S REPORT NUMBER(S) NOLTR 72-38 9b. OTHER REPORT NO(S) (Any other numbers that may be assigned this report)	

10. DISTRIBUTION STATEMENT

Approved for public release; distribution unlimited.

11. SUPPLEMENTARY NOTES	12. SPONSORING MILITARY ACTIVITY Chief of Naval Material Washington, D. C. 20360

13. ABSTRACT

A double-pass schlieren photographic system was used to determine the location of laminar-turbulent transition in the wake of 22-degree half-angle sharp cones. The measurements were conducted at $M_\infty = 9.0$ over a range of Reynolds numbers from 1.5×10^4 to 1.5×10^5. Transition distances from 7 to 200 body diameters were observed. The data are compared with wake transition results previously obtained at the Naval Ordnance Laboratory and other laboratories.

DD FORM 1 NOV 68 1473 (PAGE 1)

S/N 0101-807-6801

UNCLASSIFIED

Security Classification

14 KEY WORDS	LINK A		LINK B		LINK C	
	ROLE	WT	ROLE	WT	ROLE	WT
ballistics range schlieren photography transition, wake turbulence						

WAKE TRANSITION DATA BEHIND 22-DEGREE HALF-ANGLE CONES AT M_∞ = 9.0

Prepared by:
Charles J. Infosino and Robert A. Leverance

ABSTRACT: A double-pass schlieren photographic system was used to determine the location of laminar-turbulent transition in the wake of 22-degree half-angle sharp cones. The measurements were conducted at $M_\infty = 9.0$ over a range of Reynolds numbers from 1.5×10^4 to 1.5×10^5. Transition distances from 7 to 200 body diameters were observed. The data are compared with wake transition results previously obtained at the Naval Ordnance Laboratory and other laboratories.

NAVAL ORDNANCE LABORATORY
SILVER SPRING, MARYLAND

NOLTR 72-38 21 January 1972

WAKE TRANSITION DATA BEHIND 22-DEGREE HALF-ANGLE CONES AT $M_\infty = 9.0$

This project was funded under the Independent Research Program at the Naval Ordnance Laboratory, Task Number MAT-03L-000/ZR011-01-01.

The authors are indebted to Zigurds Levensteins for the many stimulating discussions on the subject of wake transition, to Alex Longas for his assistance in setting up the electronic instrumentation associated with the schlieren, and to Gaither Boliek for making the models and sabots and keeping the Aerophysics Range smoothly operating during the course of the program.

ROBERT WILLIAMSON II
Captain, USN
Commander

a. E. Seigel

A. E. SEIGEL
By direction

CONTENTS

	Page
INTRODUCTION.	1
BACKGROUND.	2
TEST INSTRUMENTATION.	3
DATA ANALYSIS	5
COMPARISON OF DATA.	6
CONCLUSIONS	7
REFERENCES.	9
APPENDIX A.	A-1

ILLUSTRATIONS

Figure	Title
1	Variation of Transition Distance with Reynolds Number in Wakes
2	Expected Location of Turbulent Breakthrough and Inviscid Wake Breakup
3	Double-Pass Schlieren System
4	Schlieren Photo at 99 Torr; $(X/D)_T \sim 5.7$
5	Schlieren Photo at 60 Torr; $(X/D)_T \sim 10$
6	Schlieren Photo at 40 Torr; $(X/D)_T \sim 24$
7	Schlieren Photo at 30 Torr; $(X/D)_T \sim 39$
8	Schlieren Photo at 25 Torr; Turbulent Wake; $(X/D)_T < 52$
9	Schlieren Photo at 20 Torr; $(X/D)_T \sim 50\text{-}70$
10	Schlieren Photo at 13 Torr; $(X/D)_T \sim 131$
11	Schlieren Photo at 10 Torr; Laminar Wake; $(X/D)_T > 176$
12	Transition Distance, X/D (Body Diameters), Versus Body Reynolds Number, Red_∞, for NOL 22-Degree Cone
13	Transition Distance, X/D (Body Diameters), Versus Body Reynolds Number, Red_∞, Data Normalized to $M_\infty = 9.0$
14	Transition Distance, X/D (Body Diameters), Versus Body Reynolds Number, Red_∞, for NOL 22-Degree Cone
15	Transition Distance, X/D, Versus Body Reynolds Number, Red_∞, for spheres

ILLUSTRATIONS (continued)

Figure	Title
16	Sphere Data of Figure 16 Graphed in the Form X/D Versus PD
17	Transition Distance, X/D, Versus Body Reynolds Number, Red_∞, for Slender Cones
18	Transition Distance, X/D, Versus Body Reynolds Number, Red_∞, for Wide Angle Cones
19	Comparison of Transition Distance for Slender and Wide Angle Cones in Same Mach Number Range
20	All Cone Models Graphed in the Form X/D Versus PD to Show Mach Number Dependence
21	Estimate of Mach Numbers Dependence in Range $2 < M_\infty < 20$ for Cone Data Given in Figure 21 (PD = 400 Torr - mm)
22	Graph of Transition Reynolds Number Versus Mach Number from Reference (5)

TABLE

Table	Title
I	Shot Record

LIST OF SYMBOLS

d, D	Model base diameter
t, T	Transition point
P	Pressure (in torr)
x, X	Downstream wake distance from base of model
ρ	Air density
V	Free-stream velocity
μ	Viscosity
M_∞	Free-stream Mach number
Red_∞	Free-stream Reynolds number based on model diameter
Rex_∞	Free-stream Reynolds number based on the downstream distance x
$Rex_{\infty M}$	Free-stream Reynolds number based on the downstream distance x at the actual experimental Mach number
$Rex_{\infty 9}$	Same as above, but experimental Mach number is normalized to $M_\infty = 9.0$

INTRODUCTION

Transition is the term used to describe the change in a high-speed fluid from a smooth regular state (laminar flow) to a state characterized by a random, almost chaotic, fluctuation of the fluid particles about some mean values (turbulent flow).

At low speeds, fluid dynamicists have established a criterion called the Reynolds number given by $\frac{\rho V d}{\mu}$ to describe the state of the flow. Below some critical value of the Reynolds numbers, the flow remains laminar, while above the value, turbulent flow would be expected.

To establish the laminar turbulent boundary for high-speed flow such as that found in missile or re-entry body wakes, the Mach numbers, as well as the Reynolds numbers, must be specified. Even this does not suffice, however, as a number of different parameters may be used to define the Reynolds number. Thus, one may choose to use the diameter of the body, the length of the body, the downstream distance from wake neck to the transition point, or the wake width as the characteristic length. One can also use the free-stream velocity, the local wake edge velocity, or the velocity defect just before transition as the proper velocity. Most fluid dynamicists agree that the proper Reynolds number is one based on local conditions in the wake just before transition takes place. For practical use in re-entry phenomenology, such a criterion loses properties in the wake. These properties can be obtained only through difficult direct measurements or through crude flow field calculations. It is for this reason that experimentalists have found it more convenient to use a Reynolds number based on free-stream conditions, but it must be kept in mind that this criterion alone will not completely correlate the wake transition data of radically different shapes, sizes, and flight conditions.

Qualitatively, the movement of the laminar-turbulent transition point in the wake as a function of the flight environment may be described as follows. For a given model configuration and Mach number at very low pressures, the entire wake is laminar. As the pressure is increased, transition first appears far back in the wake, perhaps several hundred body diameters. The further back in the wake, the more difficult it is to locate precisely, as transition under these circumstances takes place very slowly. As the pressure is further increased, the transition point, or more precisely, transition region, moves in closer to the body and unfolds more abruptly.

Transition continues to move closer to the body until it approaches the neck region. There it stays lodged or "sticks" as the pressure is further increased until conditions are such that it finally jumps to the boundary layer. Transition behind blunt bodies, for a given set of free-stream conditions, is located closer to the neck than the wake transition behind slender bodies at the same free-stream conditions. Transition is a function of the free-stream Mach number, at least for low Mach numbers ($M_\infty < 15$).

The location of the transition point is important, not only to fluid dynamicists concerned with the nature of laminar-turbulent flow, but to the space and defense communities as well. The latter are engaged in tracking ballistic missiles during re-entry into the earth's atmosphere. Radar signals backscattered from re-entry wakes depend on fluctuations in the electron density and, hence, on the development of turbulence in the wake. Experimental data on transition have been supplied using large-scale bodies in field tests and small models in wind tunnels and ballistics ranges. The latter tests have primarily relied on optical devices (schlieren photography); though to a lesser extent, radar and probe techniques have been successfully employed.

The determination of the exact location of transition from schlieren photographs obtained in the laboratory is difficult. The inherent scatter in the data requires repeated identical test runs to pin down the location. In many cases, the photographs are of such low contrast that a fair amount of subjective judgement is required in taking measurements from the photographs. This is especially true at low pressures where not only is the contrast low but changes take place rather slowly, i.e., over many body diameters. In addition, the numbers of parameters which affect transition are numerous. The model size and shape, pressure, Mach number, and angle of attack appear to be the most important.

BACKGROUND

The literature on wake transition studies is extensive. The first ballistics range measurements were conducted in 1962 by R. E. Slattery and W. G. Clay (reference (1)) at Lincoln Laboratories. They reported wake transition data behind model spheres at velocities 4,000 and 8,000 feet per second and behind 12-1/2-degree cones at 3,000 and 5,500 feet per second. Their range pressure was varied from 10 to 200 torr.

Additional experimental studies were undertaken at the California Institute of Technology (references (2) and (3)), the AVCO Corporation (references (4) and (7)), the Naval Ordnance Laboratory (NOL) (references (6) and (8)), General Motors Defense Research Laboratory (GMDRL) (references (9), (10), and (12)), and Arnold Engineering and Development Center (reference (13)). This work covered a wide range of model configuration and aerodynamic conditions. The general trend of the published data and the location of transition downstream in the wake are sketched in Figure 1.

Some of the most significant work on wake transition was conducted by Wilson at GMDRL (references (9), (10), and (12)). In a report on the far-wake behavior of hypersonic spheres in 1967, Wilson introduced the concept of "breakthrough" to explain certain inconsistencies in far-wake sphere data reported earlier. Briefly, the near-wake may be decomposed into two parts; an inner viscous wake generated by viscous interaction with the body and an outer "inviscid" or entropy wake generated by the detached shock at the nose of the body. As expected, at high Mach numbers, the viscous inner wake goes turbulent only a short distance from the neck. This transition cannot be observed with a schlieren photographic system, since it is masked by the high-temperature outer wake. The turbulent inner wake grows rapidly and eventually "breaks through" the edges of the surrounding outer wake. This is what is observed on the schlieren and mistakely recorded as transition. It is important to note, however, that this phenomenon only applies to high Mach number blunt-body wakes. Wilson also reported the observation of turbulence, or more properly, laminar instabilities, in the wake far downstream (>1000 body diameters) at low Reynolds numbers, i.e., at conditions below which one would not expect the wake to go turbulent. The transition location, as pictured by Wilson, can be sketched as shown in Figure 2.

The purpose of this report is to add more experimental data to the already extensive, but often confusing and sometimes contradictory information published during the last ten years. It was felt that the far-wake region behind cone models at low Reynolds numbers was important and had not been explored. This project was funded under the Independent Research Program at NOL, Task Number MAT-03L-000/ZR011-01-01. The tests were conducted in the Aerophysics Range at NOL using a sensitive double-pass schlieren system.

TEST INSTRUMENTATION

The Aerophysics Range at NOL is 5 inches in diameter and 300 feet long. The double-pass schlieren system used to take pictures of the wake was located 100 feet from the launcher. Shadowgraph pictures before and after the schlieren were used to estimate the angle of attack of the cone models. The high-quality schlieren mirror was 12 inches in diameter and had a focal length of 180 inches. The mirror was mounted approximately 2-1/2 inches from the flight axis inside a special pipe section. The optical path was enclosed in a 2-foot-diameter, 15-foot-long pipe. It was necessary to "fold" the optical path because of the limited room size perpendicular to the range. A diagram of the system is shown in Figure 3. A time-delay circuit activated by the spark shadowgraph station in front of the schlieren was used to delay the firing of the schlieren until the section of wake of interest was in the field of view. Since all models were 1/4-inch base diameter, 48 body diameters of wake could be seen at one time.

Variations in the velocity from shot to shot, random scatter in the transition location, and guesswork as to the approximate

location of transition forced us to fire many rounds to find the transition point at each range pressure. This was especially true at the lower pressures where transition was located far back in the wake and only gradually unfolded. All launches ascertained to have a large angle of attack were rejected. Because of these problems, in order to obtain sufficient data, a powder-gun launcher was used rather than the more complicated light-gas gun. The powder gun limited the program velocity to a maximum of 11,000 feet per second, but allowed us to launch as many as ten shots a day.

The models, with one exception, were made of solid aluminum. They were 1/4-inch base diameter 22-degree half-angle cones with just a slight amount of nose bluntness ($R_N/R_B \sim .08$). For protection during launch, the models were enclosed in a five-piece lexan sabot (four fingers and a base cap).

The velocity for these tests varied from 9,000 to 11,000 feet per second, and the range pressure was adjusted from 10 to 100 torr. Simple calculations indicated that even at the most severe heating condition (11,000 feet per second and 100 torr), the aluminum cones would not reach their melt temperature until after they had passed the schlieren station 100 feet downrange.

Schlieren pictures of wakes at pressures from 100 to 10 mmHg are shown in Figures 4 through 11. Both vertical and horizontal schlieren knife edges were used. The term transition, as used in this report, refers to the first noticeable disturbance or instability in a laminar wake. Only at high pressures could a definite point be located. In some cases, the first instability appeared to be damped out for several body diameters before appearing again. When this happened, a range of values for transition was recorded. At high pressures, transition appeared abruptly and was located close to the body. Full turbulence developed almost immediately.

At low pressures, transition was more gradual and not easily defined. Most of the pictures at 10 and 15 torr revealed either a completely laminar wake or a turbulent wake, i.e., the actual transition point or region was not observed. Transition could only be assumed to have taken place somewhere in the region bracketed by the completely laminar or turbulent results.

For models at an angle of attack in the vertical plane, the shock waves (from the bow and wake neck) were asymmetrical. The greater the angle of attack, the greater the asymmetry. In such cases, transition first appeared on the side of the wake in which the nose of the model was pointing. The fluctuations at the wake edge were initially low in amplitude and very periodic. The periodicity remained for many body diameters before full random turbulence set in.

The data shots used to establish the location of transition are listed in Table I. The angle of attack was estimated primarily

from the two-view shadowgraph station just in front of the schlieren. Asymmetry in the vertical profile of the shock waves observed on the schlieren pictures correlated quite well with the vertical angle of attack determined from the shadowgraph station in front of the schlieren. An attempt was made to evaluate the effect of angle of attack on the location of transition, but this was not successful, as the data were too scattered. All shots with a large angle of attack were simply discarded. The column labeled $(X/D)_9$ means that the transition distance was shifted slightly in value in order to normalize the data to a common Mach number, in this case, Mach 9.

DATA ANALYSIS

Unreduced data are shown in Figure 12. The Mach number for these points varied from 8 to 10. The low Reynolds number data were obtained at a range pressure of 10 torr, and the high Reynolds number data were obtained at a range pressure of approximately 100 torr. Some of the data points represent transition for models with a slight angle of attack at the schlieren station, but in no case were these models at an angle of attack greater than 5 degrees. A vertical line is drawn through several of the data points. In such cases, the exact beginning of transition could not be determined from the photographs. Transition seemed to take place over an extended region, for example, from 40 to 52 body diameters for the one test run recorded at Red_∞ equal to 6.6×10^4 (~ 40 torr).

Figure 13 shows the same data normalized to a common Mach number. This was achieved by using the transition data correlation for cones and wedges provided by Zeiberg (reference (5)). The exact procedure is given in Appendix A. Most of the points were only slightly shifted in the process. This graph, however, emphasizes what appears to be a break in the slope of the data at Red_∞ equal to 2.5×10^4. This is more clearly seen in Figure 14 where bars are used to represent the best estimation of the range of transition suggested by the previous data. Each bar subjectively takes into account the added weight that should be given those shots with zero angle of attack and the added weight that should be given to a cluster of transition points in a given region rather than the outermost points. This plot should be considered the main data graph.

A straight line of slope -1 can be drawn through the scatter bars for Red_∞ values 2.5×10^4 to 10^5. This is the linear region where Rex_∞ is independent of body Reynolds number, i.e., Rex_∞ = const. = 1.8×10^6. At 99 torr, the data fall below this slope, i.e., transition takes place closer to the body (5 to 7.5 body diameters). This might be considered an ablation effect, i.e., at high pressure the aluminum cone ablates, thus triggering transition in the wake early. Note, however, that one of these cones, in fact, the one that gave transition closest to the body, was a titanium model. Titanium has a higher melting temperature than aluminum and, thus, would be expected to ablate less than aluminum at the same flight conditions. If ablation effects are present, one would expect

transition in the case of a titanium cone to occur further downstream with respect to the transition point of aluminum cones, but this is not the case.

The data definitely change slope at a Reynolds number below 2.5×10^4. This is probably the viscous damping region. Most of the points used to determine the transition region at 10 torr indicated a laminar wake. If anything, then this "point" should be higher, thus emphasizing the indicated change in slope even more.

Three pictures of turbulent wakes not fully turbulent, but wakes whose appearance would more aptly be described as resembling a twisted rope, were obtained about 1000 body diameters back at a pressure 7 torr ($Red_\infty \sim 1.15 \times 10^4$). No measurements were taken from these pictures, however, as the cone models in all three cases were at severe angles of attack.

Several additional features of the data should be mentioned. It is not clear whether part of scatter in transition location might be due to angle-of-attack effects, in spite of the fact that only those shots with very small angles of attack were used. In most instances, however, those shots with small angles of attack gave or indicated a transition point further back than those shots determined to have zero angle of attack, contrary to the fact that angle of attack should induce early transition. This fact adds to the evidence that there is random scatter in the transition data rather than some bias due to, for example, angle of attack. On the other hand, if transition is affected by some parameter such as the rate of change of angle of attack, then this could affect (bias) the data, especially at the higher pressures where the oscillation rate is higher. We did not have any way to determine this during the program.

COMPARISON OF DATA

Transition data on spheres reported on by researchers at Lincoln Laboratories (reference (1)) and GMDRL (reference (9)) are shown in Figure 16. The data points indicated in Figure 16 were based on points read from the graphs given in the indicated references. When necessary, the original data were cast in the form X/D versus Red_∞ using additional parameter information supplied in these references, such as the model size or velocity. The lines drawn through the data are our own best fit to these points. The Lincoln data at $M_\infty = 7.1$ were obtained using three different size spheres; 1/8, 1/4, and 1/2 inch. There does not seem to be a size dependence, at least not within the scatter of the data. Similarly, the results obtained using 5- and 15-mm spheres show no size dependence. There is only a weak Mach number dependence. This is shown more clearly in Figure 17 where X/D is plotted against PD (pressure times diameter). Referring again to Figure 16, the Lincoln data follow a slope of -1.4, thus indicating that Rex_∞ is not constant, but depends on Red_∞. The GMDRL data (slope -1) does not show this dependence, nor will the cone data which follow.

]1

The Lincoln data at $M_\infty = 7.1$ also show a drastic change of slope just below $Red_\infty = 3 \times 10^4$. This is due to viscous damping as noted earlier. Lincoln sphere data at $M_\infty = 17 - 18$ published in a separate paper (reference (11)) were not included in this plot as the values measured were reported by Wilson (reference (12)) to be a measure of "breakthrough" rather than transition.

Slender cone data from Lincoln Laboratories (reference (1)), GMDRL (reference (12)), and NOL (references (6) and (13)) are plotted in Figure 18. By slender cone, it is meant cones with half angles less than 15 degrees and little if any nose bluntness ($R_N/R_B < 0.1$). At high Mach numbers, the slender cones show a stronger Mach number dependence than the spheres. All slopes were determined to be -1. This implies Rex_∞ = const. over the range of data given. The 10-degree slender cone data obtained at AVCO (reference (7)) showed too much scatter to be included in the graph.

Finally, wide-angle cone data are given in Figure 19. The cones chosen all have half angles ≥ 15 degrees and bluntness ratios $R_N/R_B < 0.1$. This includes selective data from AVCO (reference (7)), GMDRL (reference (9)), and the present NOL results. Note well the excellent argument between the AVCO wide-angle cones and the NOL 22-degree cones at $M_\infty = 9.0$. The NOL data extend the data into the very low Reynolds number regime (1.5×10^4). Measurements of transition were taken as far back as 200 body diameters.

A composite plot based on the data given for the slender and wide-angle cones in the region $M_\infty = 9.0$ to 13.0 is shown in Figure 20. The graph reveals that the NOL 6.3-degree cone at Mach 9.1 and the NOL 22-degree cone data at Mach 9.0 are almost perfectly matched, at least in the overlap region $Red_\infty = 8 \times 10^4$ to 2×10^5. This graph implies that the effect of Mach number and the scatter in transition data completely dominate any effect which one might expect to see for different cone angles. A change in the cone angle will change the local wake Mach numbers, M_e, but not very much at $M_\infty = 9.0$.

In all these graphs, the transition distance in base diameters was plotted against the free-stream body Reynolds number. This procedure results in a set of straight lines of slope -1, each line corresponding to a different Mach number. Since the body Reynolds number, Red_∞, contains the Mach number, a more meaningful graph would be a plot of X/D versus pressure times diameter. This is shown in Figure 21. In this way, the transition distance as a function of pressure and Mach numbers can be read directly.

A rough numerical estimate of the Mach number dependence for the cones can be obtained by recasting the data of Figure 21 in the form transition distance versus Mach number. The transition values were selected at PD = 400 torr mm. As shown in Figure 22, the points can be fitted with a line of slope 1.2, thus indicating a Mach number power dependence of 1.2, i.e., $(X/D)_t \propto M_\infty^{1.2}$ over the range $2.7 < M < 20$.

It is important to note that any conclusions with respect to the cone data presented here apply only to cones with little if any nose bluntness. The transition behind cones of different bluntness ratios may be widely different. This can be seen in the extreme case by comparing a cone and sphere at the same Mach number.

Finally, one must be careful when applying these results to full-scale vehicles. The data here were obtained from ballistics range tests using models of base diameters 3/16 inch to 1/2 inch, i.e., a size factor of 2.6. Extrapolation to full-scale vehicles (12 inches or larger) would be quite presumptuous.

CONCLUSIONS

1. Wake transition distances measured behind a 22-degree half-angle cone at Mach 9 agree well with the distances measured for both wide angle and slender cones in the same Mach number range. This implies that inherent scatter in the transition measurements and to a lesser extent slight differences in the free-stream Mach numbers dominate over any effect one might expect to see due to differences in cone angle.

2. Transition measurements for cones at Mach 9 are extended into the low Reynolds number regime $Red_\infty \sim 1.5 \times 10^4$.

3. The data for the 22-degree cone at Mach 9 suggest that the viscous damping regime starts at about $Red_\infty = 2.5 \times 10^4$.

4. A rough empirical estimate of the Mach number dependence for sharp cones indicates $(X/D)_t \propto M_\infty^{1.2}$ in the range $2.7 < M_\infty < 20$.

13

REFERENCES

(1) Slattery, R. E., and Clay, W. G., "Turbulent Wake of Hypersonic Bodies," ARS Preprint 2673-62, Nov 1962

(2) Demetriades, A., and Gold, H., "Correlation of Blunt-Bluff Body Wake Transition Data," Graduate Aeronautical Laboratories, California Institute of Technology, Internal Memorandum No. 12, 20 Sep 1962

(3) Demetriades, A., "Hot Wire Measurements in the Hypersonic Wakes of Slender Bodies," AIAA Journal, Feb 1964

(4) Pallone, A. J., Erdos, J. I., Eckerman, J., and McKay, W., "Hypersonic Wakes and Transition Studies," (Tasks 3.1 and 3.5 - Rest Project) AVCO Corporation, Technical Memorandum RAD-TM-63-33, 14 Jun 1963

(5) Zeiberg, S. L., "Correlation of Hypersonic Wake Transition Data," General Applied Science Laboratories Technical Report No. 382, 16 Oct 1963

(6) Lyons, W. C., Brady, J. J., and Levensteins, Z. J., "Hypersonic Drag, Stability, and Wake Data for Cones and Spheres," AIAA Journal, Vol 2, No. 11, Nov 1964

(7) Berkhoff, G., Eckerman, J., and McKay, W., "Turbulent Hypersonic Wakes," AVCO Corporation, Technical Memorandum RAD-TM-64-17, 31 Mar 1964

(8) Levensteins, Z. J., and Krumins, M. V., "Aerodynamic Characteristics of Hypersonic Wakes," AIAA Journal, Vol 5, No. 9, pp 1596-1602, Sep 1967

(9) Wilson, L. N., "Body-Shape Effects on Axisymmetric Wakes Transition," AIAA Journal, Vol 4, No. 10, pp 1741-47, Oct 1966

(10) Wilson, L. N., "Far Wake Behavior of Hypersonic Spheres," AIAA Journal, Vol 5, No. 7, pp 1234-38, Jul 1967

(11) Clay, W. G., Lambett, M., and Slattery, R. E., "Measured Transition from Laminar to Turbulent Flow and Subsequent Growth of Turbulent Wakes," AIAA Journal, Vol 3, No. 5, pp 837-41, May 1965

(12) Wilson, L. N., "Far Wake Behavior of Hypersonic Blunted Cones," AIAA Journal, Vol 5, No. 8, Aug 1967

(13) Bailey, A. B., Hiatt, J., and Hayfield, D. A., "Correlation of Schlieren, Radiation, and Radar Measurements in the Far Wake of Nonablating Hypervelocity Spheres at Low Reynolds Numbers," AEDC-TR-69-183, Jan 1970

TABLE I

SHOT RECORD

Shot No.	Pressure mmHg	M_∞	Angle of Attack in Degrees Horiz./Vert.*	Photo-View**	Red_∞ X10^4	$(X/D)_t$ Measured	$(X/D)_{t9}$ Normalized		Comments
6/26/6	99	8.55	+2, -½	0-39	15.9	7.2-10	7.7-10.7	√	
6/25/8	98	8.27	x, -½	0-42	15.2	7.0	7.8	√	
7/24/9	99	8.10	+1½, +1	0-30	15.0	5.7	6.6	√	Titanium Model
8/10/2	60	8.36	-3, 0	1-49	9.4	10	11.1	√	
7/21/5	60	8.36	-7½, ½	2-50	9.4	21	23.9	?	Large Angle of Attack in Horizontal Plane
7/24/6	40	9.12	0, -1	13-61	6.85	24	23.5	√	
6/22/ 1515	41	8.65	x, +1	7-55	6.65	41-52	43-55	√	Edge Turbulent
7/14/6	41.5	8.05	+1, -2½	0-48	6.26	39	45	√	
8/10/3	40	8.54	0, 0	3.4-51.4	6.44	28-32	30-34	√	
8/11/3	30	9.24	5, 0	10.5-58.5	5.22	39	37.5	√	
7/24/2	30	9.50	x, +1	43-91	5.35	$\lesssim$40	$\lesssim$37	√	
7/24/4	30	9.34	0, -1	14-62	5.25	>62	>58.7	?	Laminar Wake
7/24/3	29.5	9.50	-8, -1	40-88	5.25	≤40	≤37	?	Large Angle of Attack in Horizontal Plane
8/11/7	30	9.33	0 , x	24-72	5.22	~32	~30	?	Poor Photo/Bow Shocks Asymmetrical
8/10/4	25	9.58	0, 0	52-100	4.49	<52	<47.5	√	Turbulent
6/19 1000	25	8.80	x, -1	0-43	4.13	>43	>44.5	√	Laminar
7/16/2	25	9.52	+5½, +2	53-101	4.46	~60	~55	?	Rough Estimate of Transition

* - X in column indicates angle could not be determined.
** - Numbers in this column indicate extent of wake in body diameters shown in schlieren photograph
√ - Good Shot
? - Questionable

TABLE I (Continued)

Shot No.	Pressure mmHg	M_∞	Angle of Attack in Degrees Horiz./Vert.*	Photo-View**	Red_∞ $X10^4$	$(X/D)_t$ Measured	$(X/D)_{t9}$ Normalized		Comments
7/14/3	25	8.14	0, -4½	23-71	3.8	35	40	?	Large Angle of Attack
7/24/7	20	9.57	-2½, 0	32-80	3.6	50-70	45-64	√	Intermittent Wake
6/24/4	20	8.22	X, +2½	2-50	3.08	~36	~40.5	?	Turbulent on One Side
7/14/8	20	8.41	+3, 0	3-51	3.15	>51	>56	√	
6/24/3	20	8.55	-3½, 2	50-98	3.21	≲50	≲53.8	√	Periodic Turbulence on One Side
7/13/1	20	9.17	X, 0	61-109	3.44	<61	<60	?	Wake All Turbulent, Poor Photo
6/24/8	15	9.28	0, -3	27-75	2.61	43 72	41-69	√	Turbulent on One Side
7/14/4	15	9.4	+5, 0	44-92	2.64	>92	>86	√	Poor Photo
7/14/2	15	9.23	-5, -3½	63-111	2.60	≲63	≲61	?	Large Angle of Attack
7/14/1	15	9.58	X, -4	76-124	2.69	<76	<70	?	Turbulent on One Side
7/13/5	15	9.64	X, 0	130-178	2.71	<130	<117	√	Too Far Back
8/14/4	15	9.29	-3½, X	40-88	2.61	>88	>84	√	Laminar >88
7/24/5	13	9.44	+2, +2	88-136	2.3	>136	>127	√	
8/28/4	13	9.40	0, 0	107-155	2.29	~131	~123	√	
6/24/10	10	9.89	+4½, +2½	100-148	1.85	>148	>128	√	
6/26/2	10	9.12	-4, +2½	194-242	1.71	<194	<190	√	Turbulent on One Side Only
6/25/3	10	9.28	0, +1	128-176	1.74	>176	>169	√	Laminar
6/25/7	10	8.27	0, 0	128-176	1.55	>176	>197	√	
7/16/4	10.5	9.46	-6½, 0	210-258	1.86	≲210	≲196	?	Angle of Attack
8/11/5	10	8.8	X, X	170-218	1.65	>218	>225	√	All Laminar

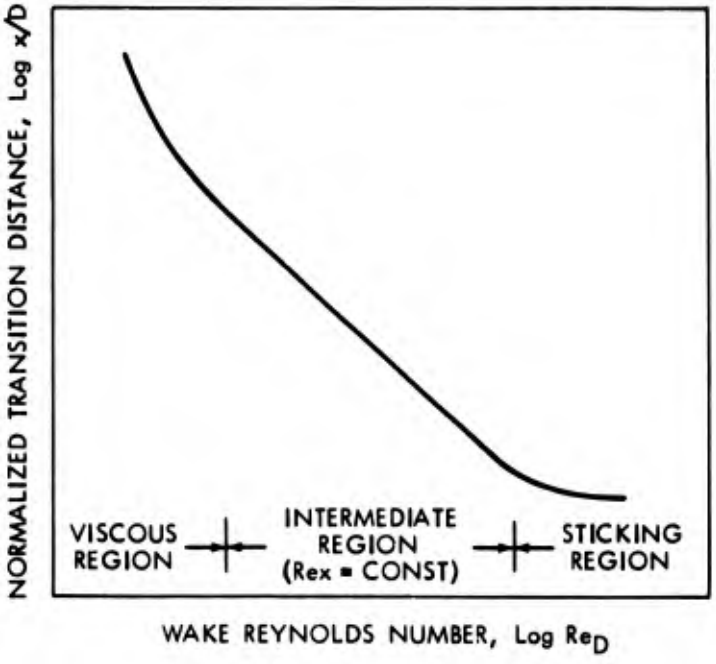

FIG. 1 VARIATION OF TRANSITION DISTANCE WITH REYNOLDS NUMBER IN WAKES (GENERAL MOTORS DEFENSE RESEARCH LABORATORY, REF. 9, FIG. 2)

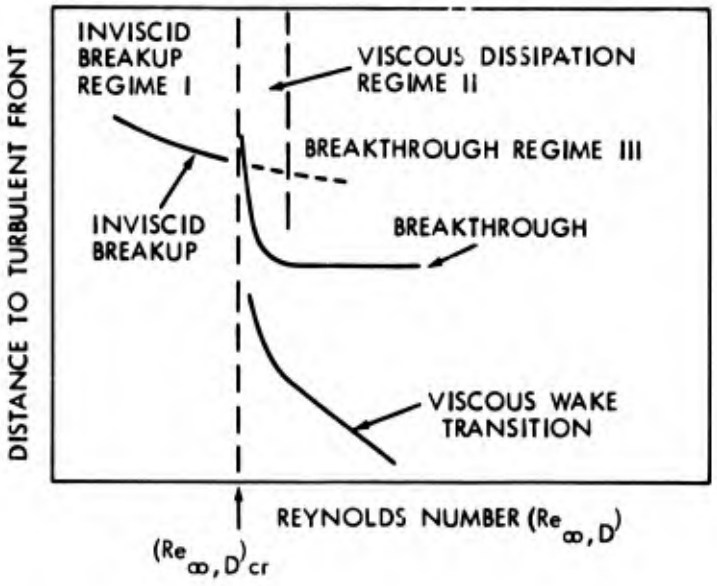

FIG. 2 EXPECTED LOCATION OF TURBULENT BREAKTHROUGH AND INVISCID WAKE BREAKUP (GENERAL MOTORS DEFENSE RESEARCH LABORATORY, REF. 10, FIG. 2)

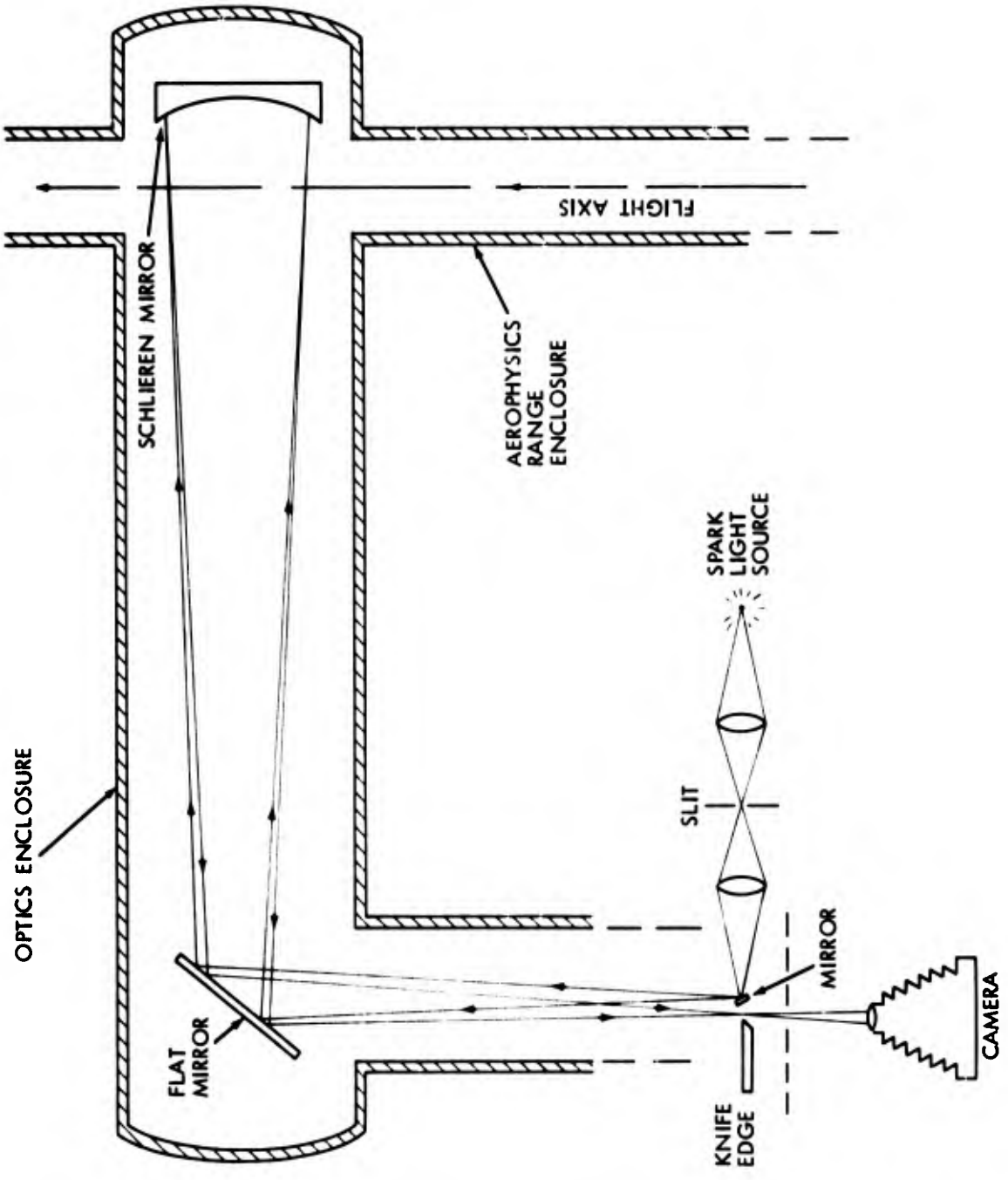

FIG. 3 DOUBLE-PASS SCHLIEREN SYSTEM

7/24/9

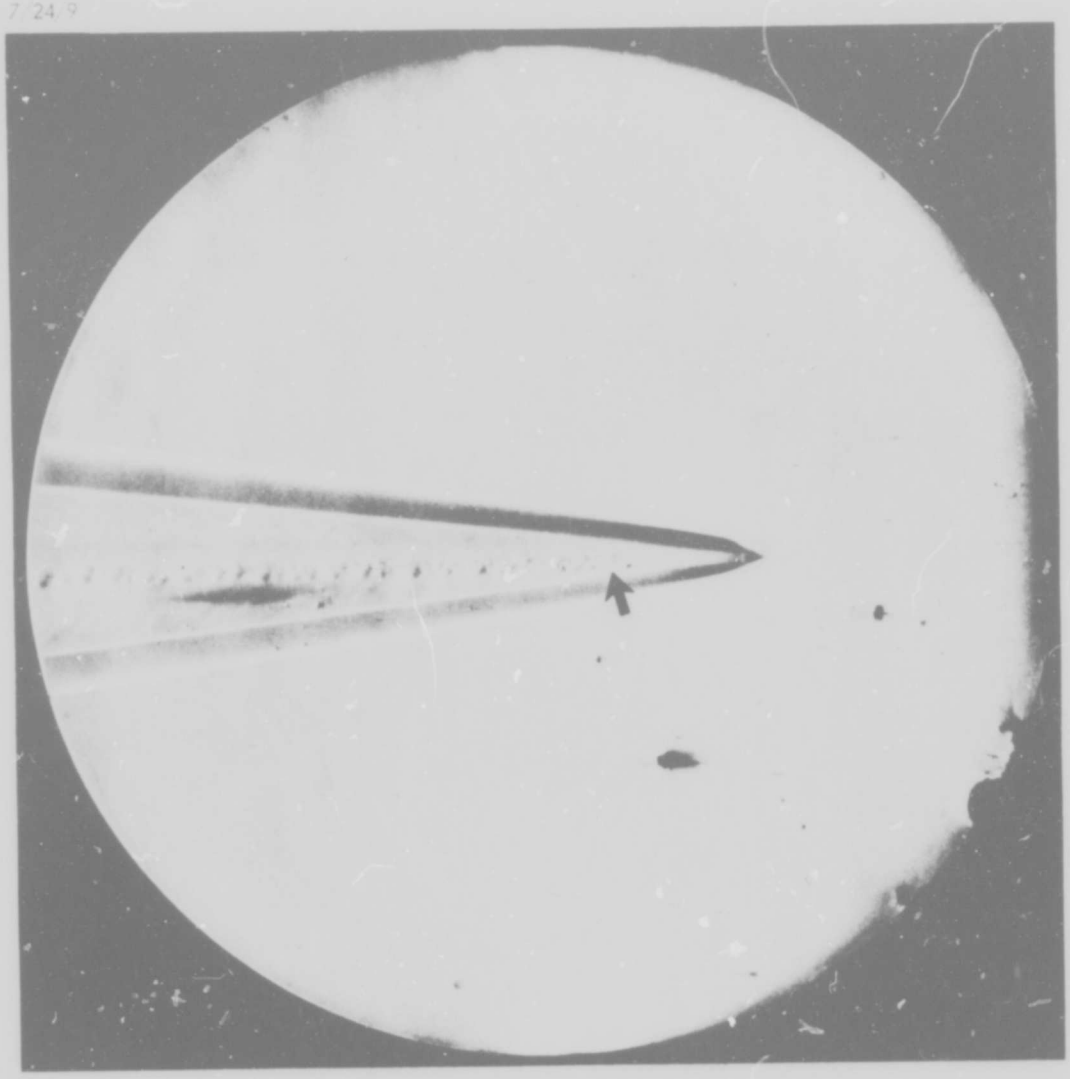

FIG. 4 SCHLIEREN PHOTO AT 99 TORR; $(X/D)_T \sim 5.7$

8/10.2

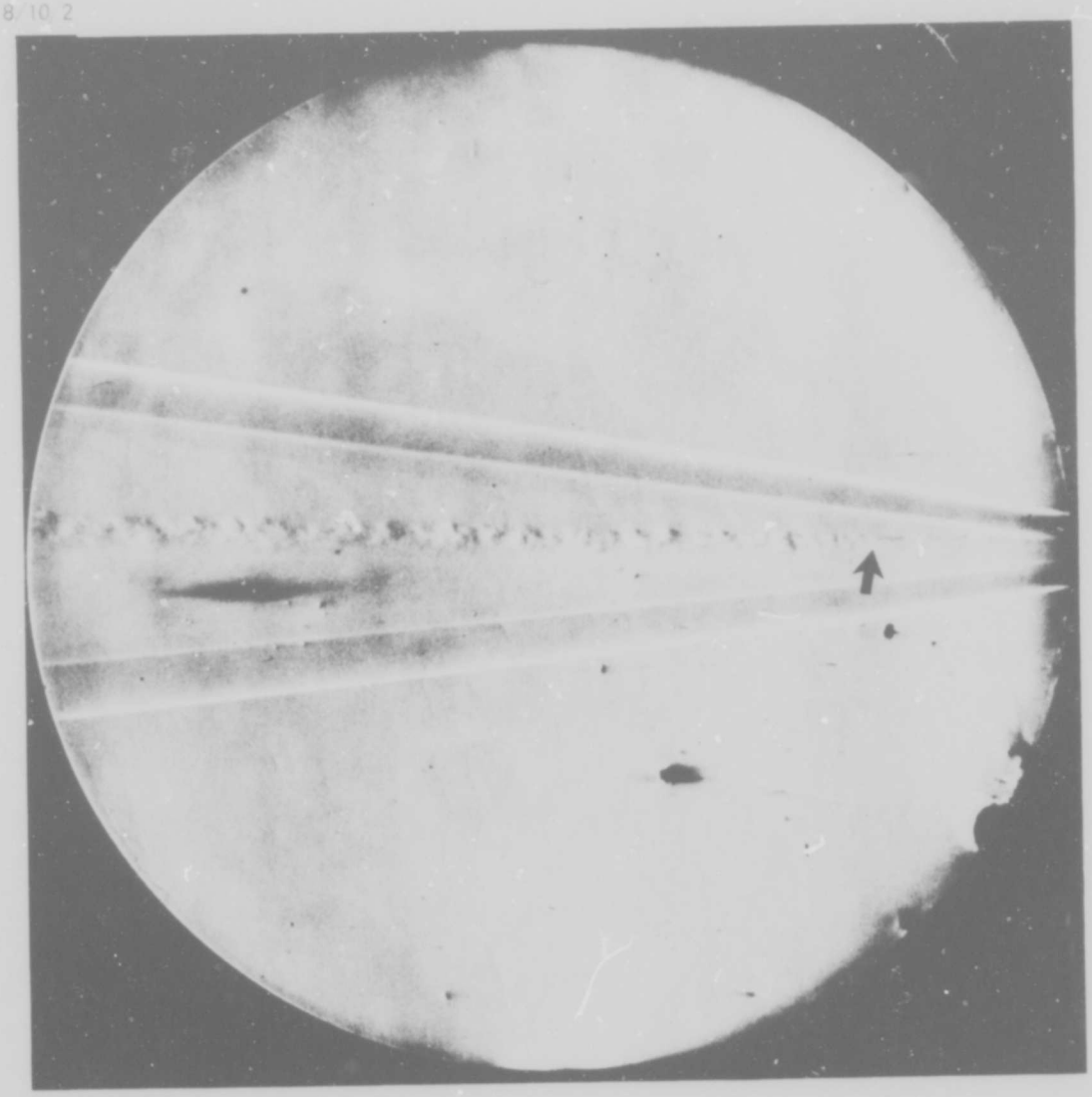

FIG. 5 SCHLIEREN PHOTO AT 60 TORR; $(X/D)_T \sim 10$

7/24/6

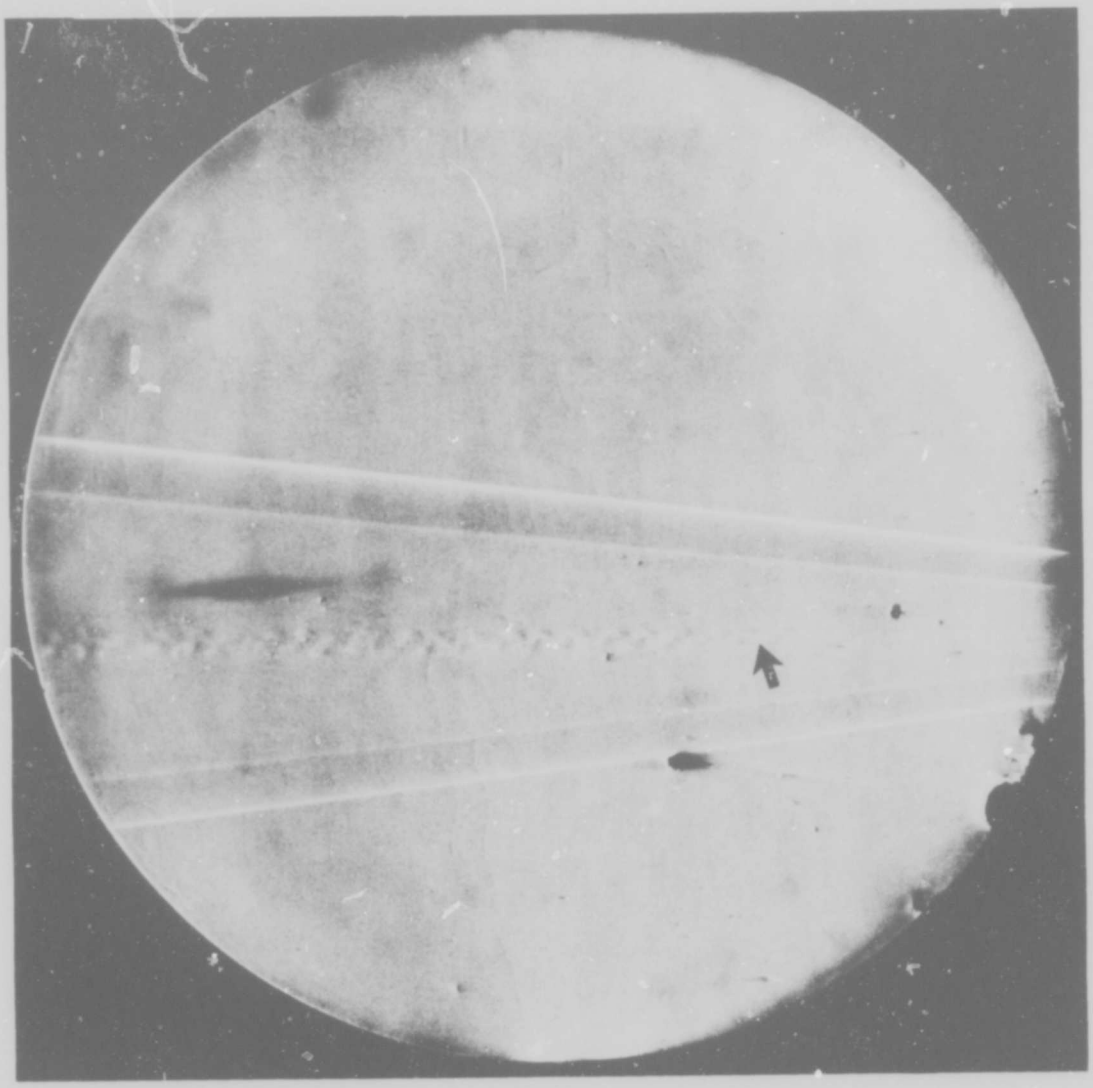

FIG. 6 SCHLIEREN PHOTO AT 40 TORR; $(X/D)_T \sim 24$

8/11/3

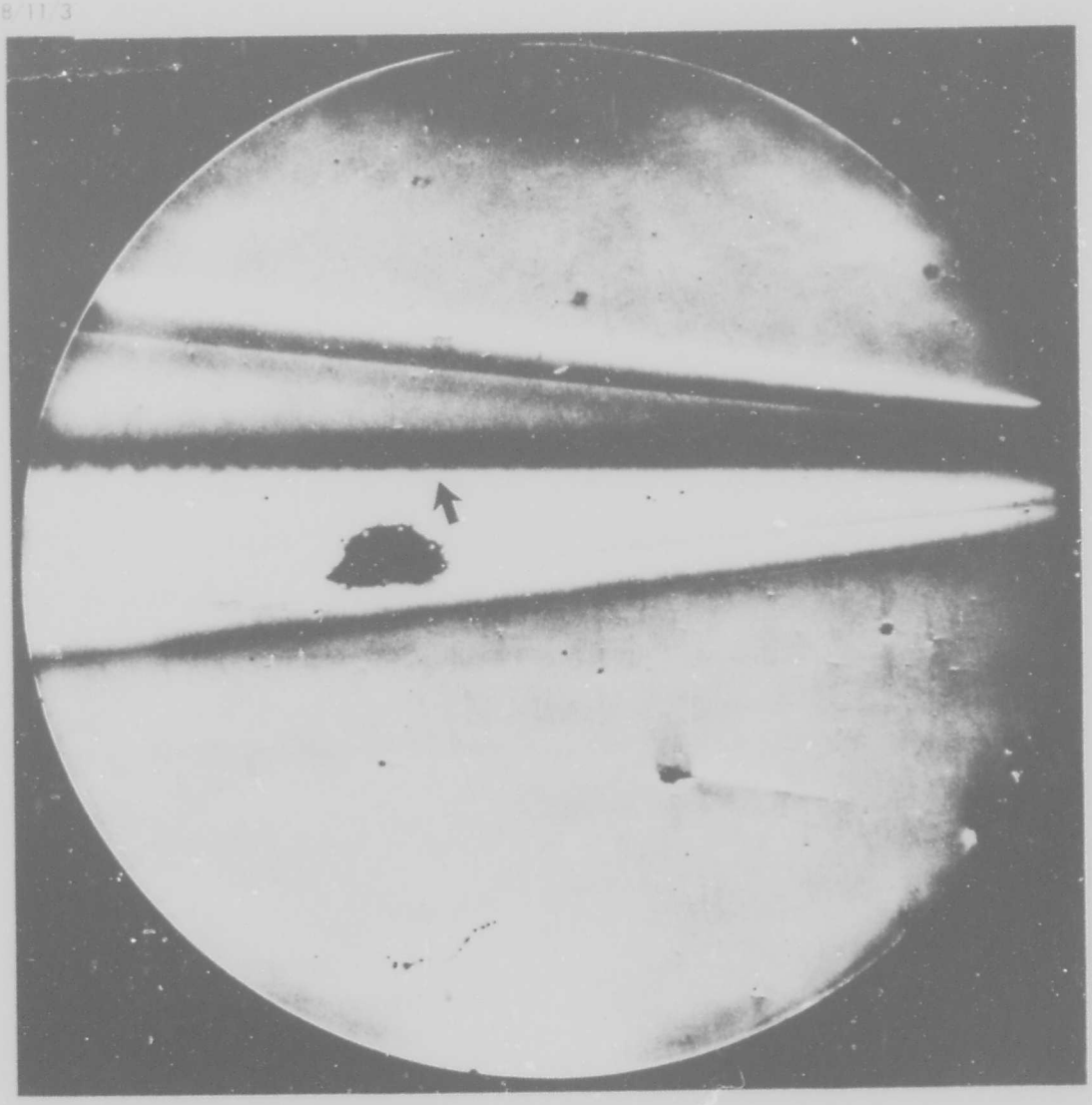

FIG. 7 SCHLIEREN PHOTO AT 30 TORR; $(X/D)_T \sim 39$

8/10/4

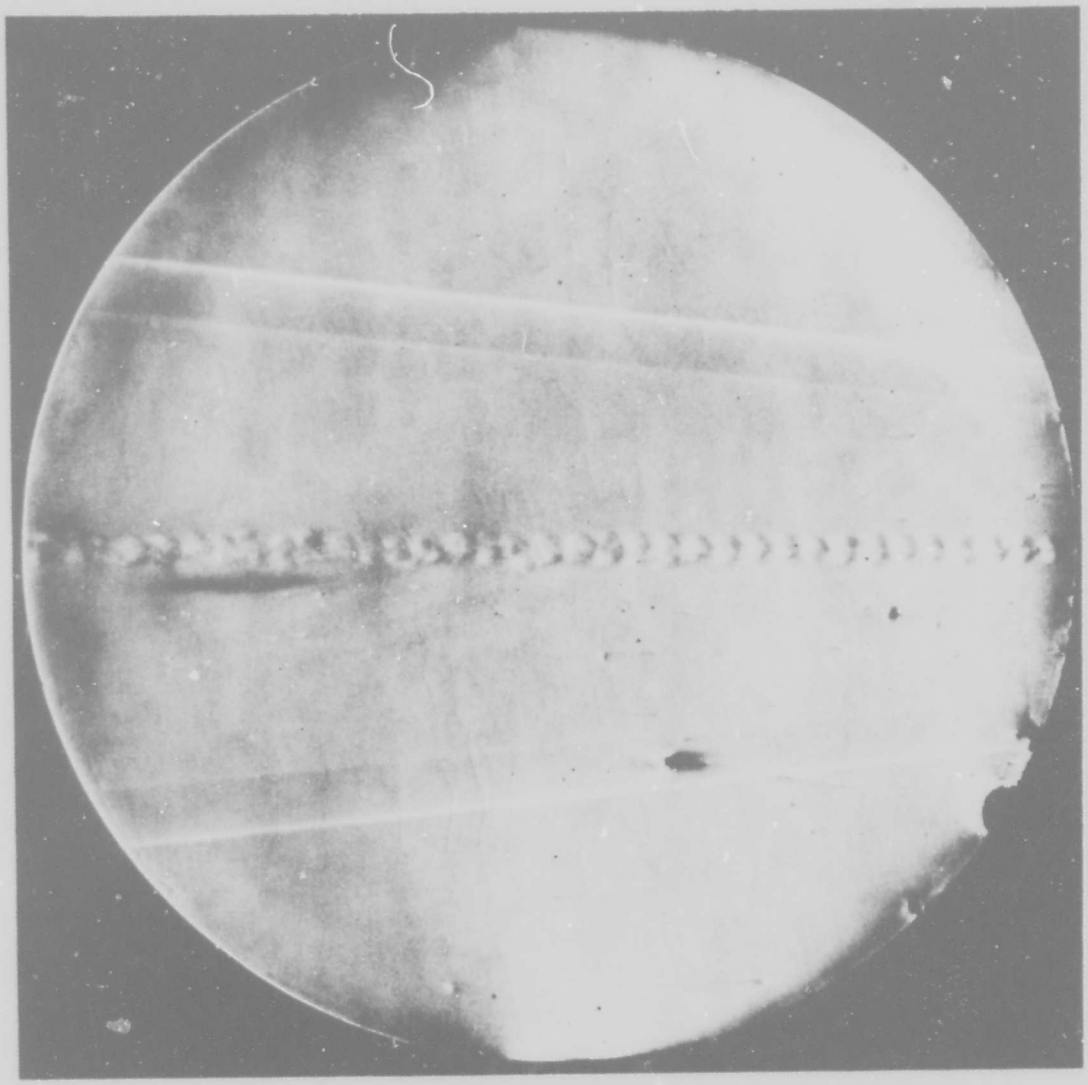

FIG. 8 SCHLIEREN PHOTO AT 25 TORR; TURBULENT WAKE; $(X/D)_T < 52$

7/24/7

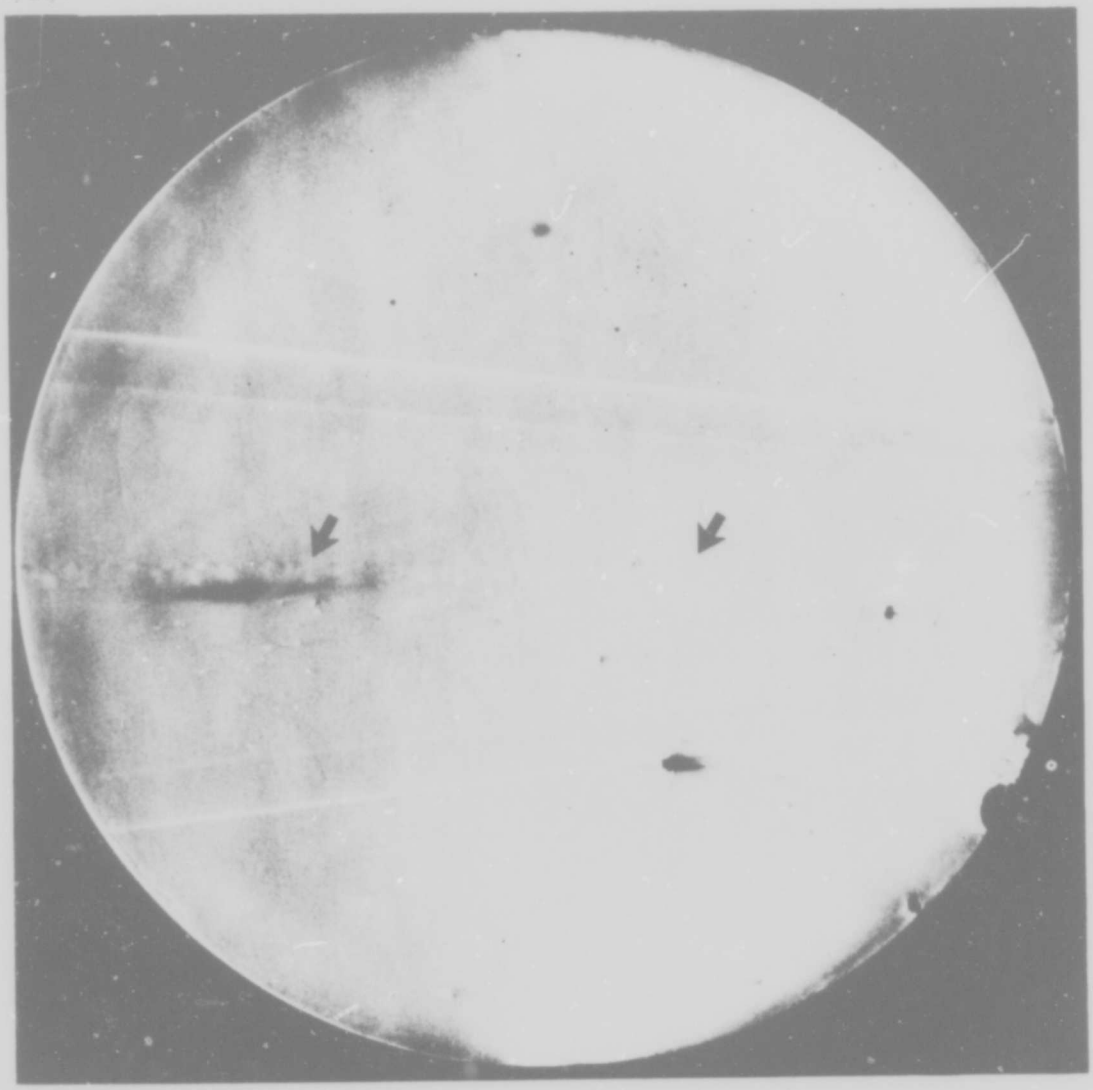

FIG. 9 SCHLIEREN PHOTO AT 20 TORR; $(X/D)_T \sim 50\text{-}70$

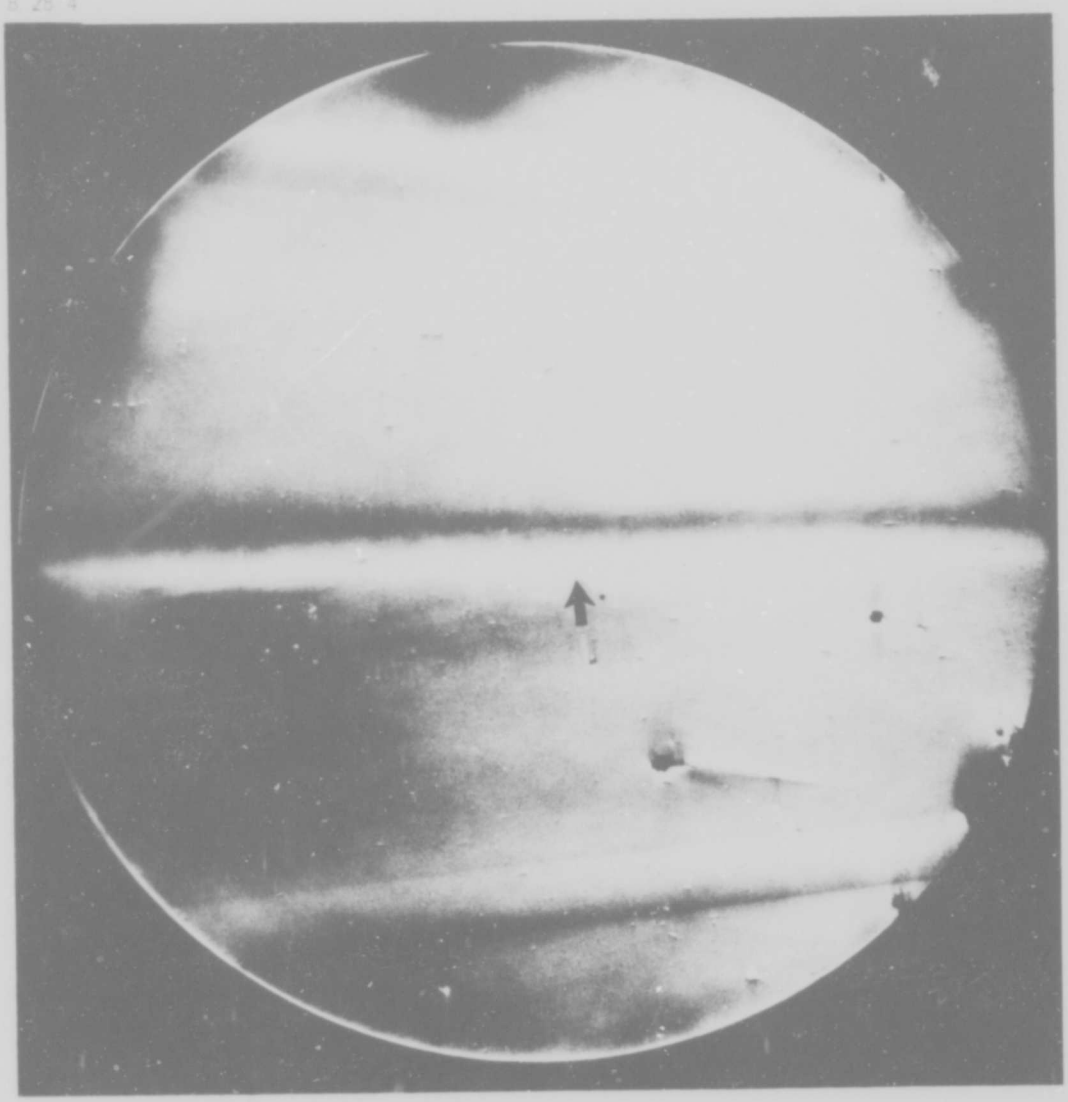

FIG. 10 SCHLIEREN PHOTO AT 13 TORR; $(X/D)_T \sim 131$

6/25/7

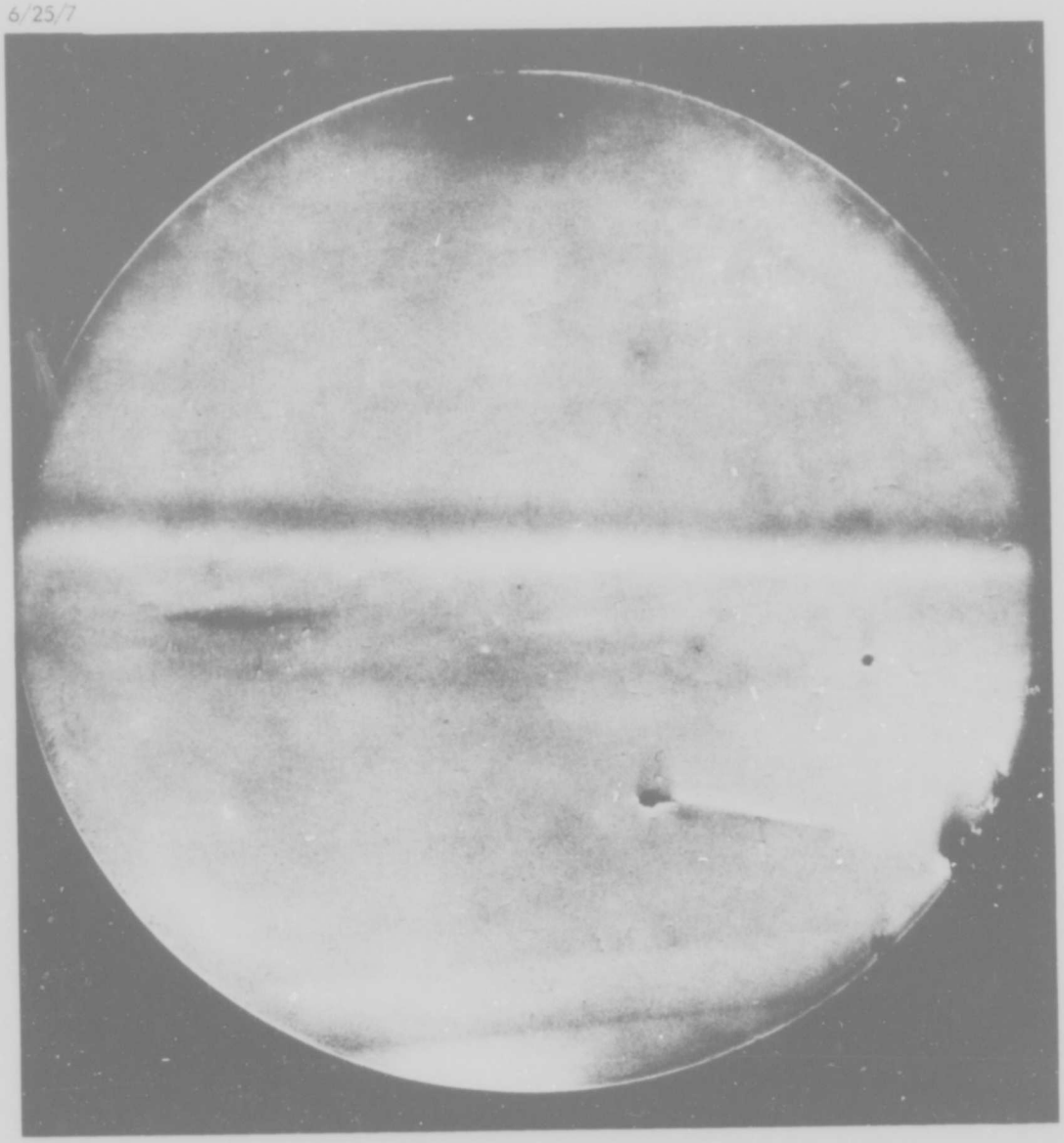

FIG. 11 SCHLIEREN PHOTO AT 10 TORR:LAMINAR WAKE; $(X/D)_T > 176$

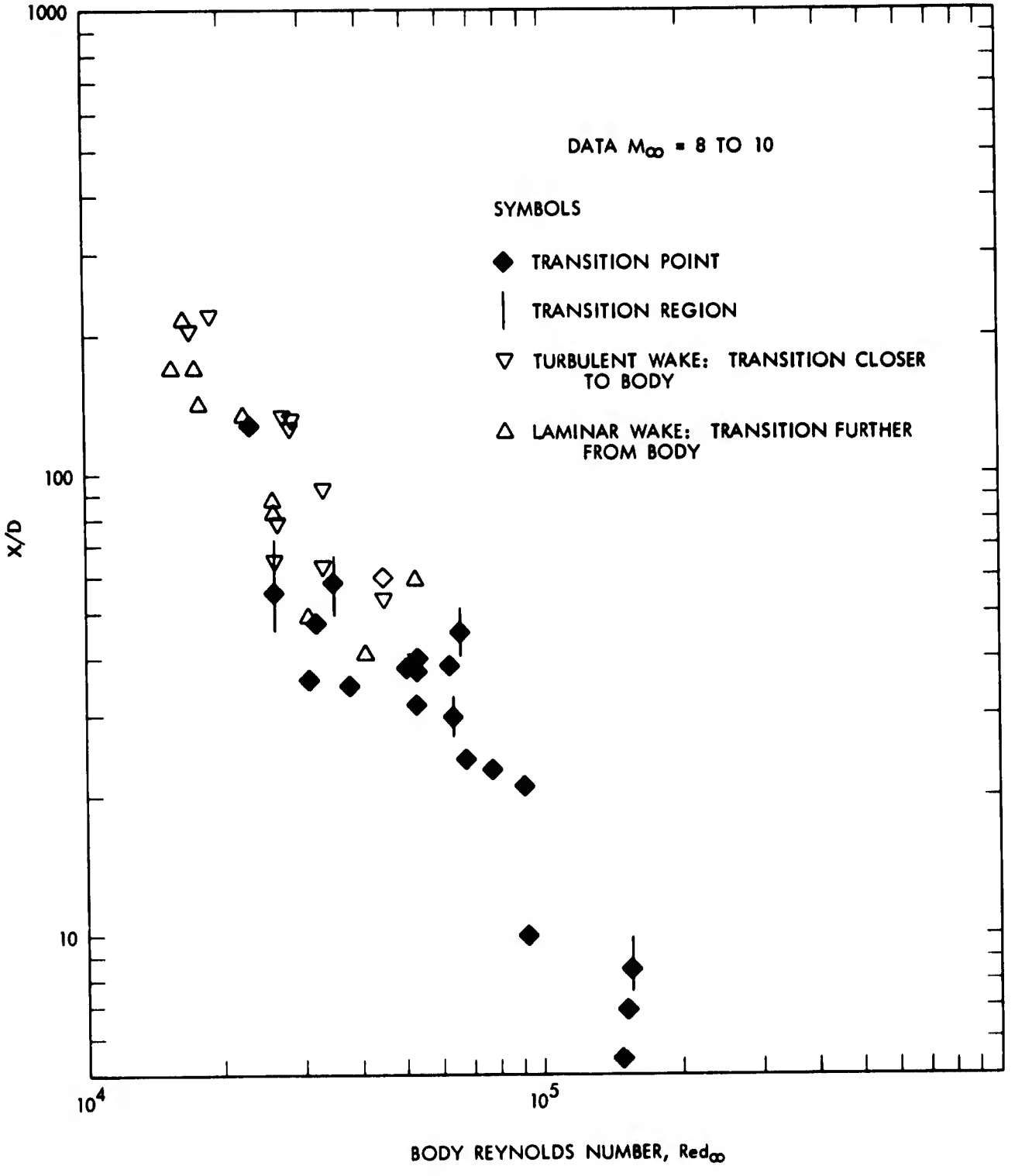

FIG. 12 TRANSITION DISTANCE, X/D (BODY DIAMETERS), VERSUS BODY REYNOLDS NUMBER, Red_∞ , FOR NOL 22° CONE

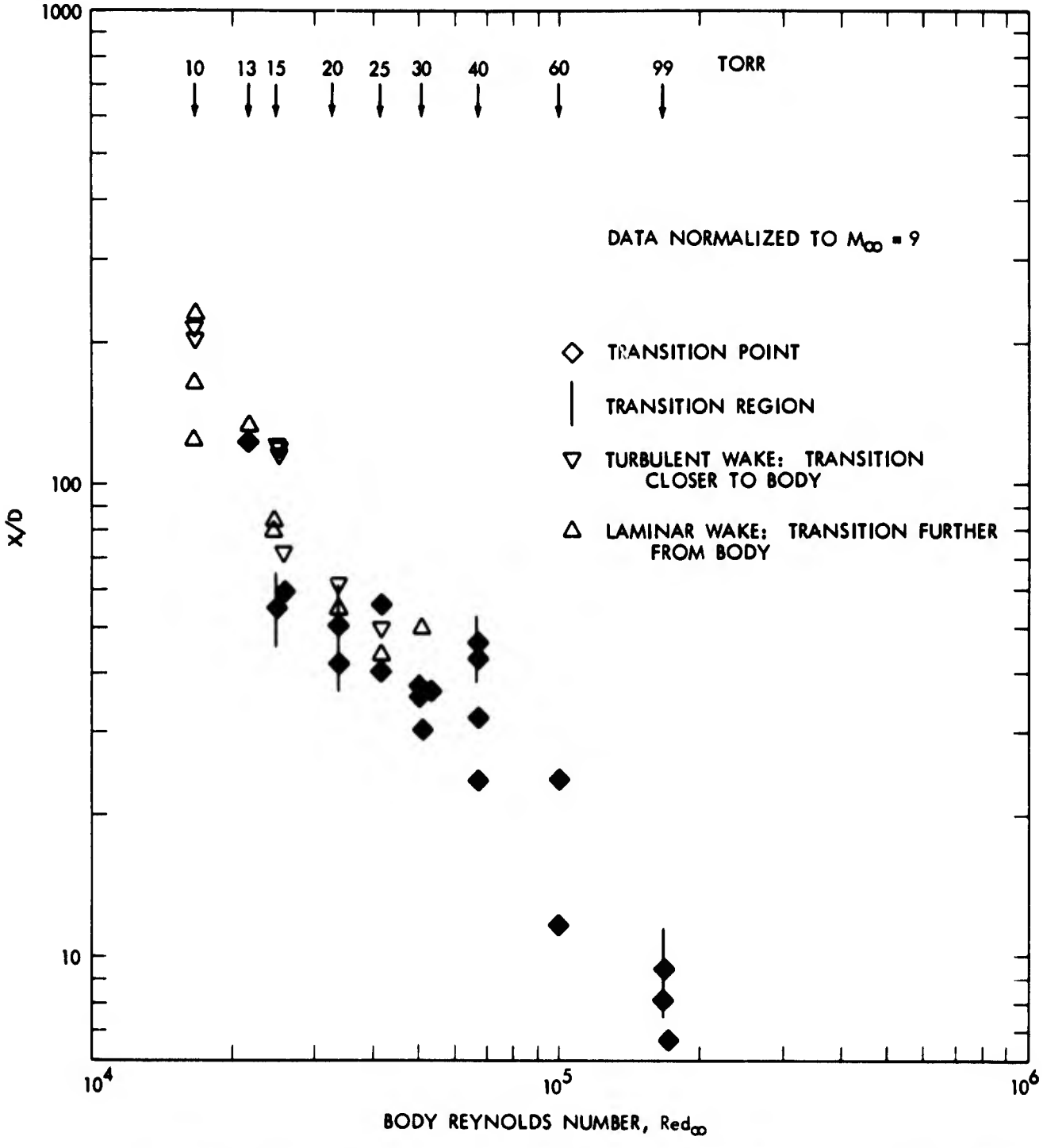

FIG. 13 TRANSITION DISTANCE, X/D (BODY DIAMETERS), VERSUS BODY REYNOLDS NUMBER, Red_∞ , DATA NORMALIZED TO M_∞ = 9.0

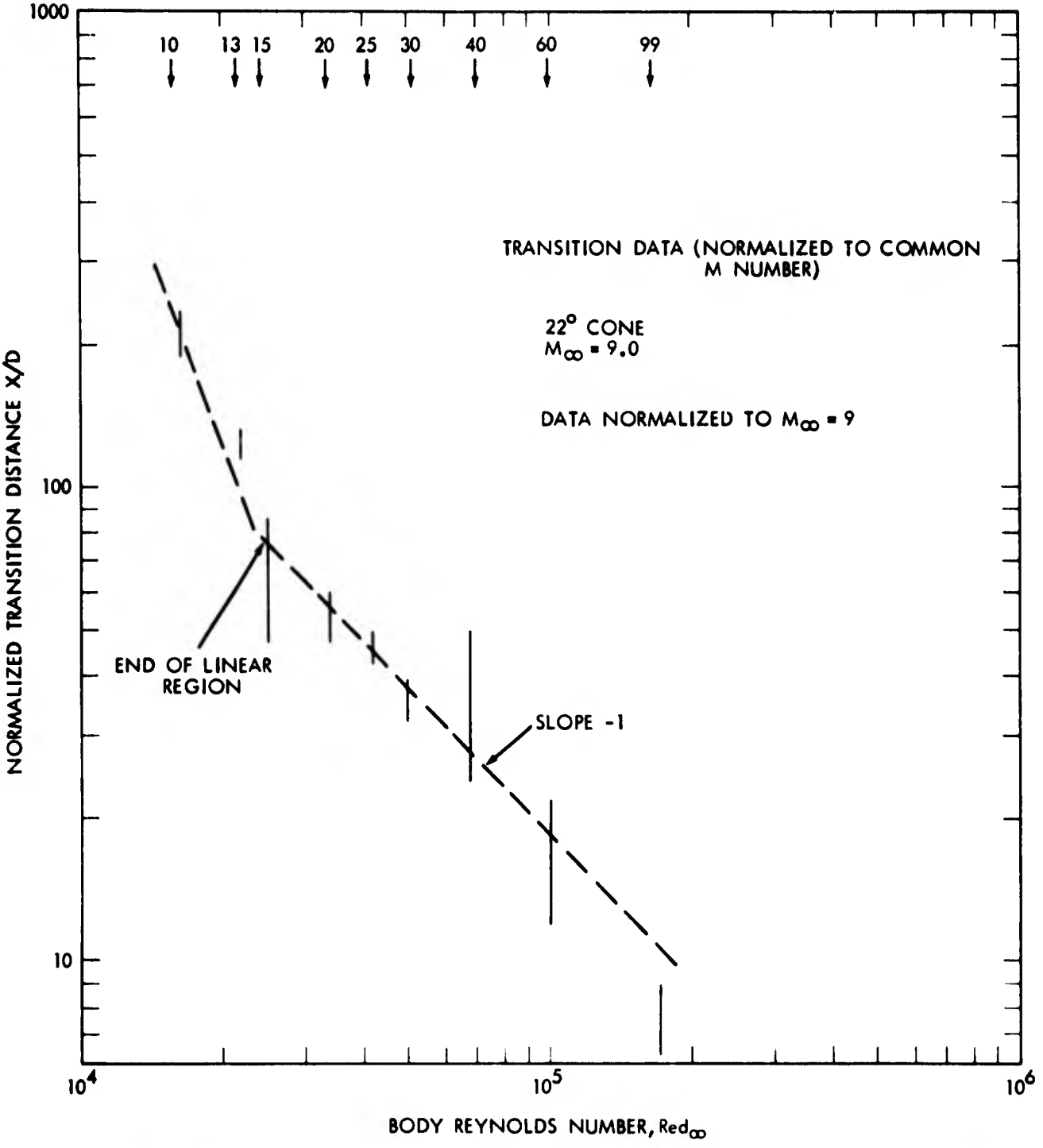

FIG. 14 TRANSITION DISTANCE X/D (BODY DIAMETERS) VERSUS BODY REYNOLDS NUMBER, Red_∞ , FOR NOL 22° CONE. DATA REPRESENTED BY BARS FOR CLARITY.

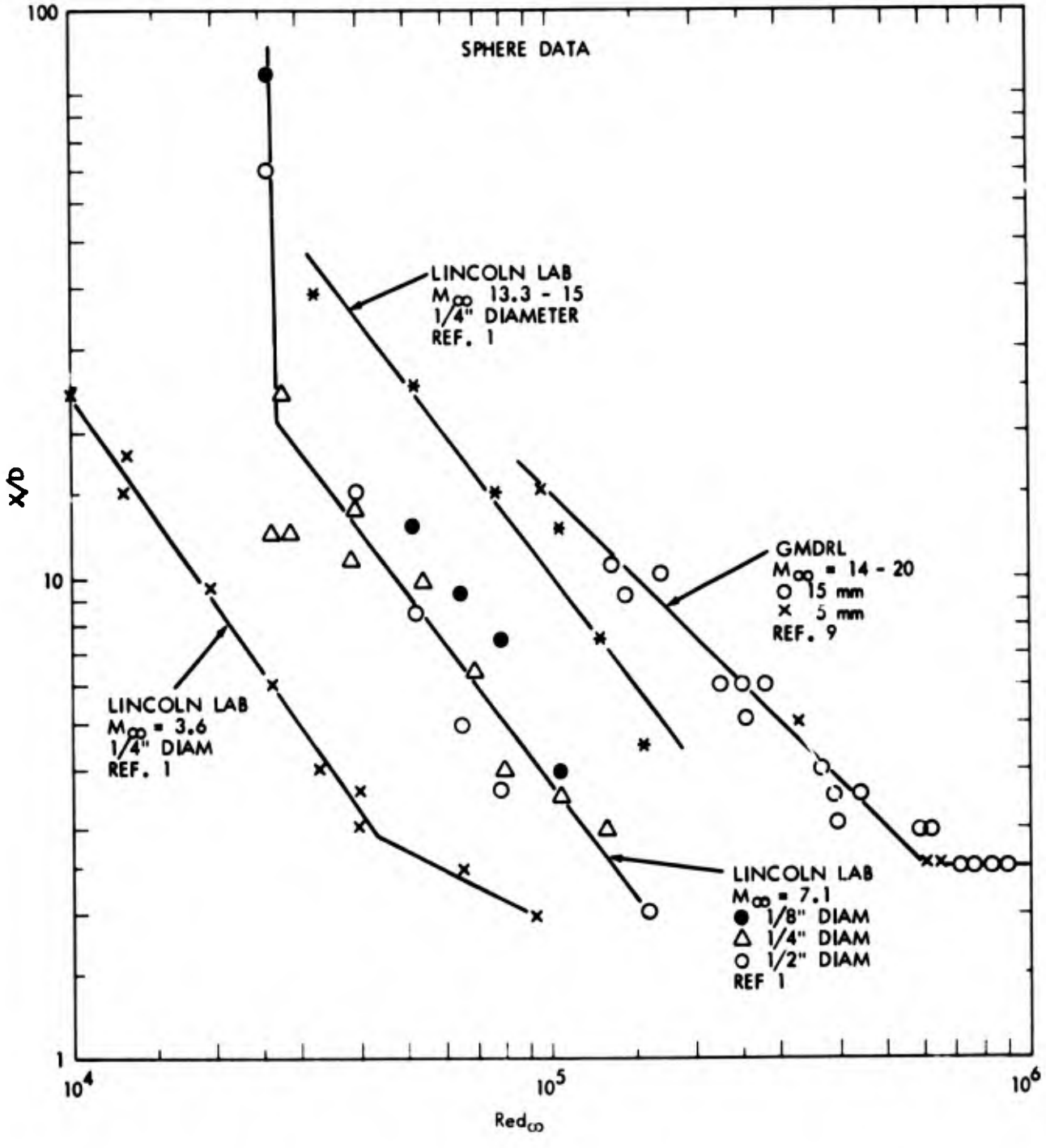

FIG. 15 TRANSITION DISTANCE, X/D, VS. BODY REYNOLDS NUMBER Red_∞ FOR SPHERES

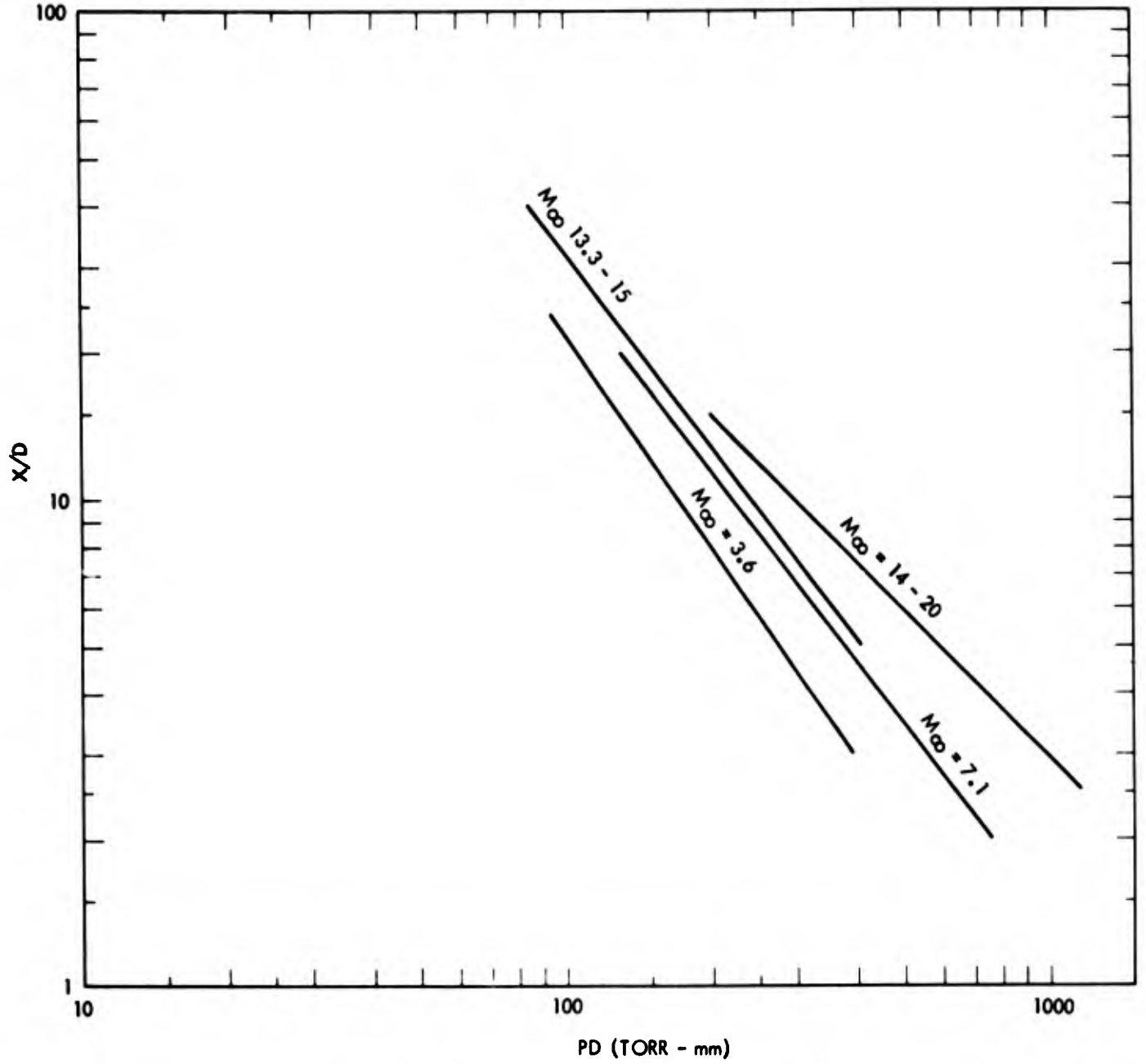

FIG. 16 SPHERE DATA OF FIG. 16 GRAPHED IN THE FORM X/D VS. PD

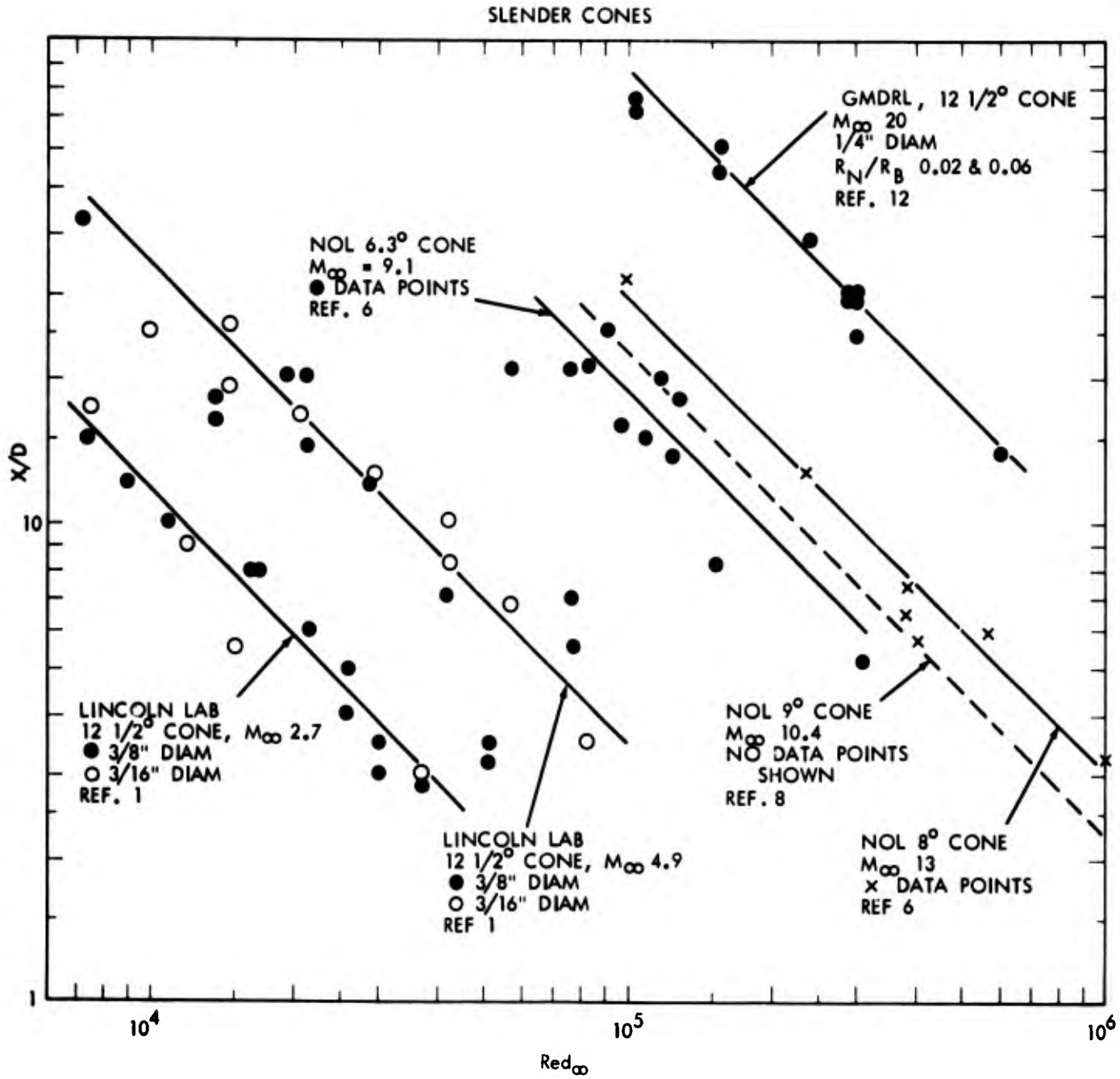

FIG. 17 TRANSITION DISTANCE, X/D, VERSUS BODY REYNOLDS NUMBER, Red_∞ , FOR SLENDER CONES

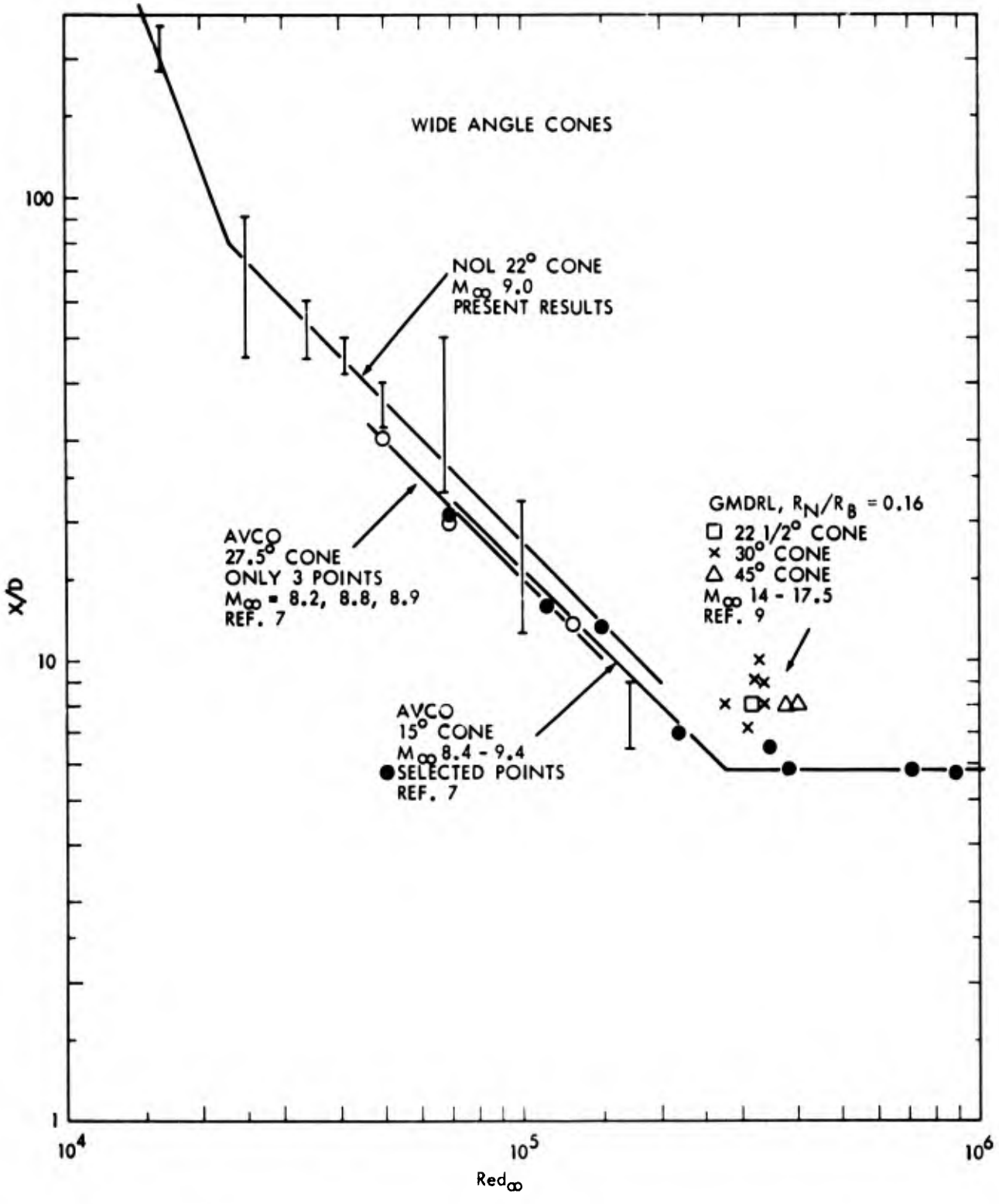

FIG. 18 TRANSITION DISTANCE, X/D, VERSUS BODY REYNOLDS NUMBER, Red_∞, FOR WIDE ANGLE CONES

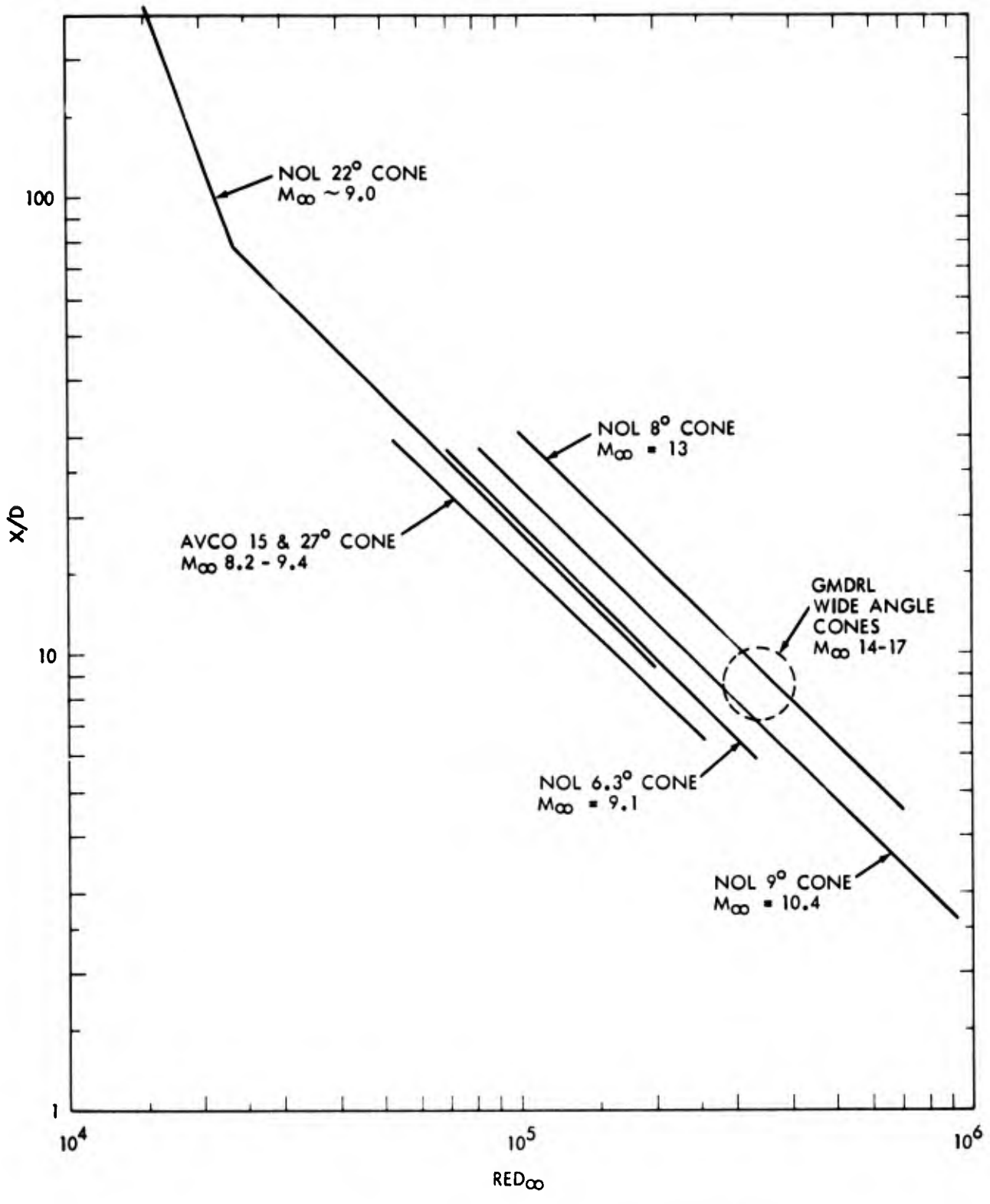

FIG. 19 COMPARISON OF TRANSITION DISTANCE FOR SLENDER & WIDE ANGLE CONES IN SAME MACH NUMBER RANGE

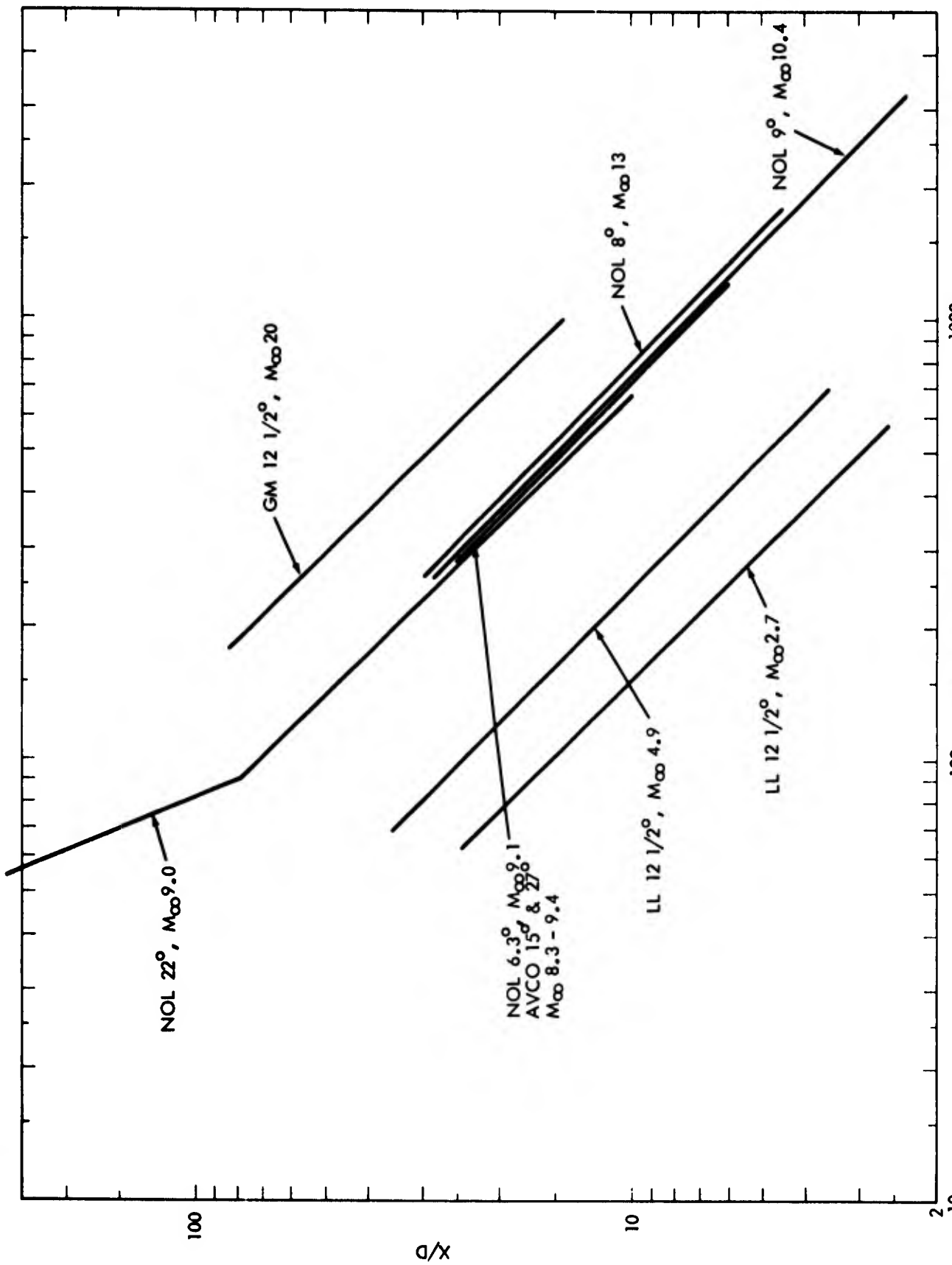

FIG. 20 ALL CONE MODELS GRAPHED IN THE FORM X/D VS. PD TO SHOW MACH NUMBER DEPENDENCE

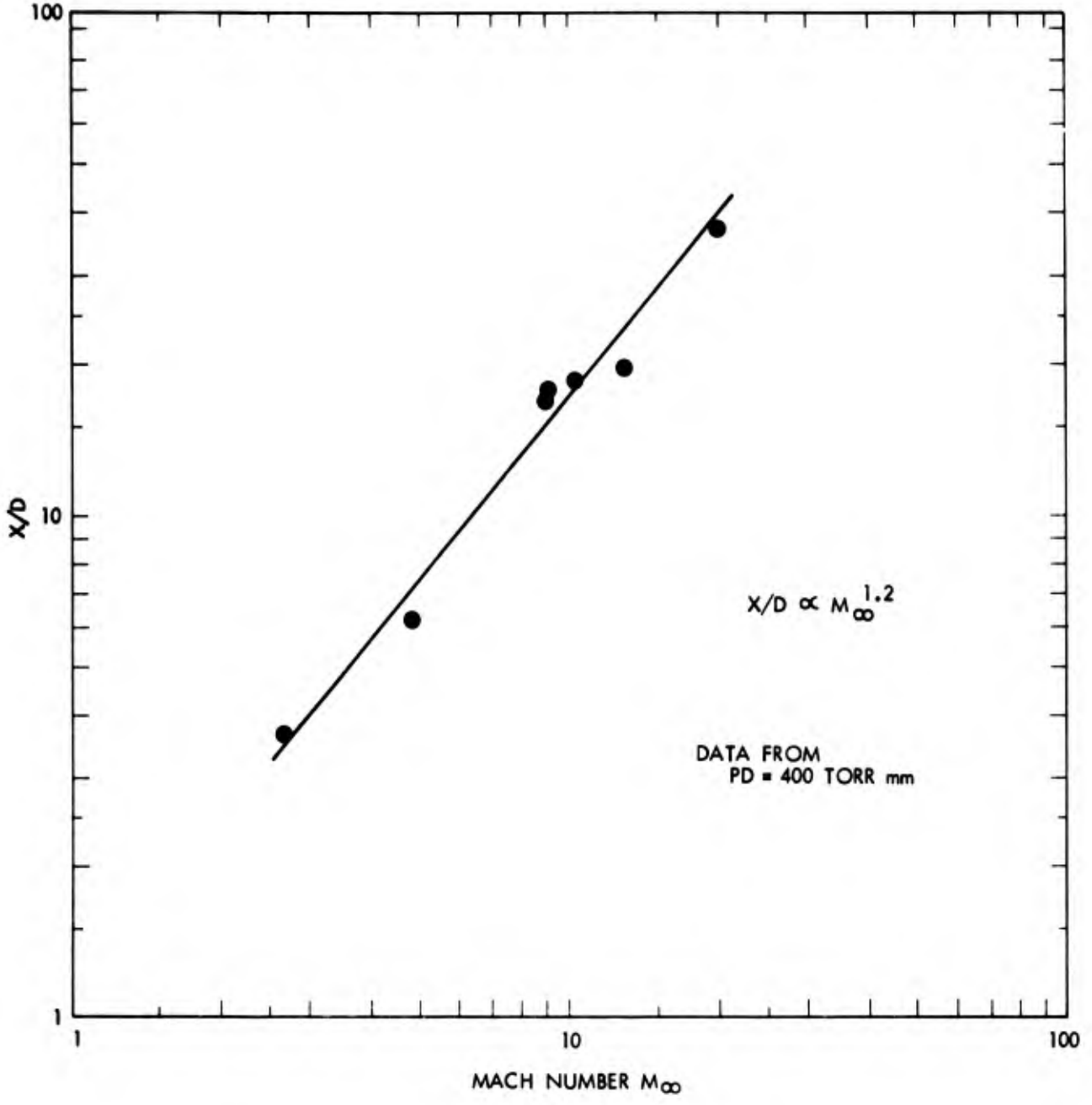

FIG. 21 ESTIMATE OF MACH NUMBERS DEPENDENCE IN RANGE $2 < M_\infty < 20$ FOR CONE DATA GIVEN IN FIG. 21 (PD = 400 TORR - mm)

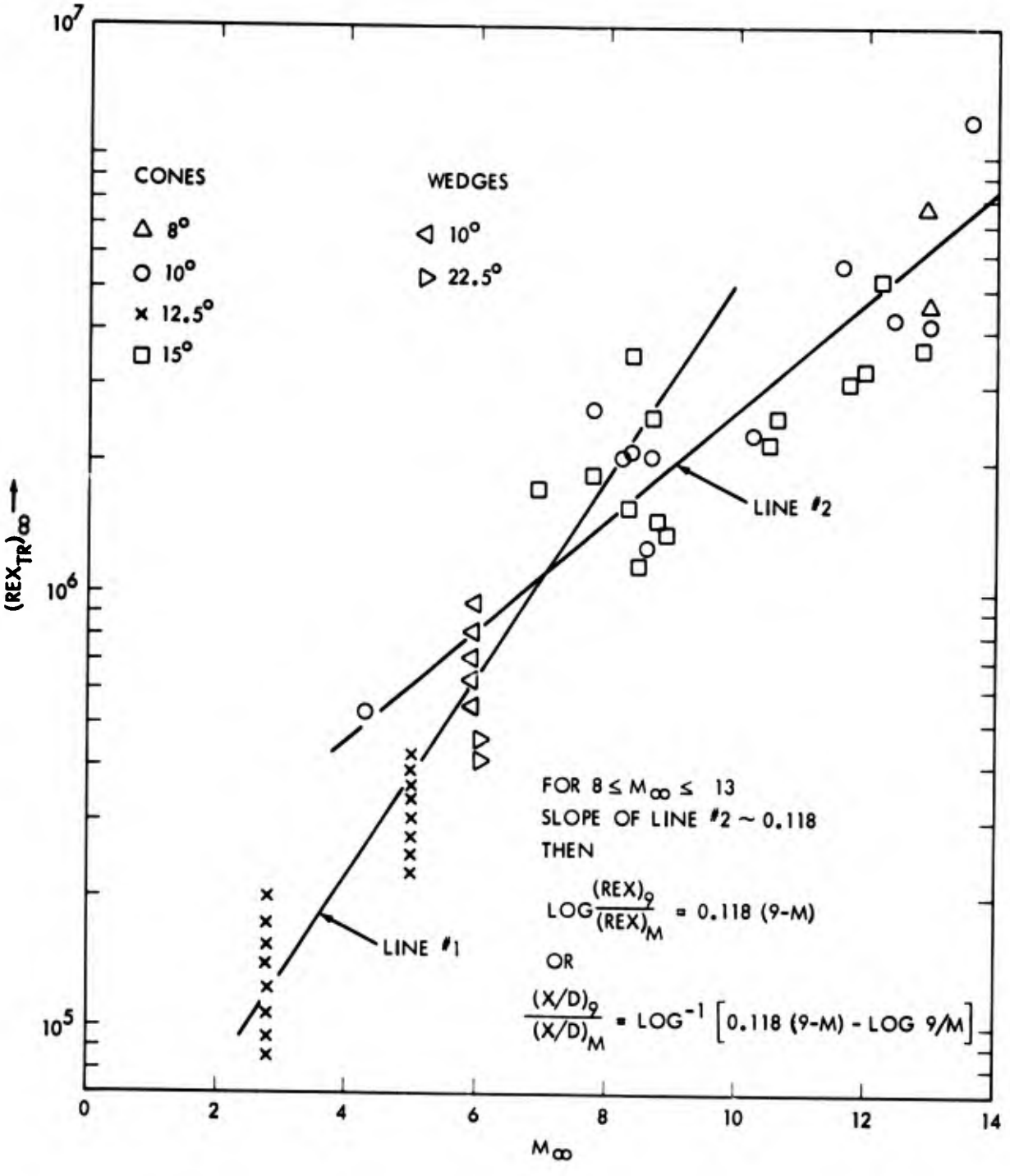

FIG. 22 APPENDIX A. GRAPH OF TRANSITION REYNOLDS NUMBER VERSUS MACH NUMBER FROM REFERENCE 5. LINE #2 SHOWN ON THIS GRAPH WAS USED TO NORMALIZE DATE IN RANGE $8 \leq M_\infty \leq 10$ TO $M_\infty = 9.0$.

APPENDIX A

Normalization of Data to Common Mach Number ($M_\infty = 9.0$)

The graph of transition Reynolds number Rex_∞ versus Mach number M_∞ is taken from reference (5), Figure 1. Between $8 < M_\infty < 13$, a straight line can be drawn through the data. The slope is approximately 0.118.

Thus

$$\log \frac{(Rex)_9}{(Rex)_M} = 0.118\ (9 - M)$$

where the symbol M represents the actual measured Mach number and 9 represents the Mach number we want to normalize to.

Since $Rex = (Red)\ (\frac{x}{d})$ and $Red \propto M_\infty$, we have

$$\frac{(\frac{x}{d})_9}{(\frac{x}{d})_M} = \log^{-1}\left[0.118\ (9 - M) - \log \frac{9}{M}\right]$$

Example:

Suppose $\frac{x}{d}$ measured to be 100 at $M_\infty = 9.5$, to normalize to Mach 9.0, we have $\frac{(\frac{x}{d})_9}{100} = \log^{-1}\left[0.118\ (9 - 9.5) - \log \frac{9}{9.5}\right]$

Thus

$$(\frac{x}{d})_9 = 92.5$$

Note: Maximum shift of data for M_∞ between 8 and 10 is ~15 percent.

DOCUMENT TRANSMITTAL
NAVAIR FORM 3900/3 (10-67)

CLASSIFICATION

UNCLASSIFIED WHEN ENCLOSURE IS REMOVED

SERIAL NUMBER (*When required*)/DATE

AD NUMBER (*To be inserted by DDC*)

ORIGINATING AGENCY

ENCLOSURE (*Report title*)

REPORT SERIES AND NUMBER

REPORT DATE

COG. NAVAIR CODE

CONTRACT/PROJECT/AIRTASK NUMBER

TO

Administrator
Defense Documentation Center for Scientific
and Technical Information (DDC)
Bldg #5, Cameron Station
Alexandria, Virginia 22314

SECURITY CLASSIFICATION

	UNCLAS	CONFI	SECRET	RD
REPORT				
TITLE OR SUBJECT				
ABSTRACT OR SUMMARY				

Enclosure is forwarded for distribution subject to limitations checked below. Request AD number be inserted in space above; two copies of this letter be returned to originating activity if shown below; two copies be sent to Commander, Naval Air Systems Command, and one copy be retained by DDC.

☐ 1. This document has been approved for public release and sale. Its distribution is unlimited.

IN ADDITION TO SECURITY REQUIREMENTS WHICH APPLY TO THIS DOCUMENT AND MUST BE MET –

☐ 2. This document is subject to special export controls and each transmittal to foreign governments or foreign nationals may be made only with the prior approval of

☐ 3. Each transmittal of this document outside the agencies of the U. S. Government must have prior approval of

☐ 4. Each transmittal of this document outside the Department of Defense must have prior approval of

☐ 5. This document may be further distributed by the holder only with specific prior approval of

SIGNATURE

TITLE

CODE

DATE

Commander Naval Air Systems Command (AIR-604)
Navy Department
Washington, D. C. 20360

CLASSIFICATION

UNCLASSIFIED WHEN ENCLOSURE IS REMOVED

S/N-0102-603-3930

GPO 872-405 C-17005